

Evaluation of Experimental Protocols for Characterizing Diffusion in Sedimentary Rocks

NWMO TR-2007-11

December 2007

P. Vilks and N.H. Miller

Atomic Energy of Canada Limited

nwmo

NUCLEAR WASTE
MANAGEMENT
ORGANIZATION

SOCIÉTÉ DE GESTION
DES DÉCHETS
NUCLÉAIRES



Nuclear Waste Management Organization
22 St. Clair Avenue East, 6th Floor
Toronto, Ontario
M4T 2S3
Canada

Tel: 416-934-9814
Web: www.nwmo.ca

Evaluation of Experimental Protocols for Characterizing Diffusion in Sedimentary Rocks

NWMO TR-2007-11

December 2007

P. Vilks and N.H. Miller
Atomic Energy of Canada Limited

Disclaimer:

This report does not necessarily reflect the views or position of the Nuclear Waste Management Organization, its directors, officers, employees and agents (the "NWMO") and unless otherwise specifically stated, is made available to the public by the NWMO for information only. The contents of this report reflect the views of the author(s) who are solely responsible for the text and its conclusions as well as the accuracy of any data used in its creation. The NWMO does not make any warranty, express or implied, or assume any legal liability or responsibility for the accuracy, completeness, or usefulness of any information disclosed, or represent that the use of any information would not infringe privately owned rights. Any reference to a specific commercial product, process or service by trade name, trademark, manufacturer, or otherwise, does not constitute or imply its endorsement, recommendation, or preference by NWMO.

ABSTRACT

Title: Evaluation of Experimental Protocols for Characterizing Diffusion in Sedimentary Rocks
Report No.: NWMO TR-2007-11
Author(s): P. Vilks and N.H. Miller
Company: Atomic Energy of Canada Limited
Date: December 2007

Abstract

Laboratory protocols have been developed, and preliminary testing has been undertaken to estimate the porosity, pore size, effective diffusion coefficients, pore water composition and permeability using archived core samples from Ordovician-aged shale and limestone formations from southern Ontario. Porosity was estimated by a water immersion technique and pore size distribution was determined using mercury intrusion porosimetry. Through-diffusion cell experiments were used to estimate effective diffusion coefficients, as well as rock capacities and effective tortuosities which provide a measure of pore geometry. Sample permeability was estimated with the High Pressure Radionuclide Migration Apparatus by pumping water through core samples under a confining pressure. In addition, thirty-day leaching experiments with deionized water were used to extract salts in accessible pore spaces for use in estimating pore fluid compositions based on sample porosity.

Archived core samples of Queenston shale and Cobourg (Lindsay) limestone were used to test the experimental protocols, and to perform a preliminary assessment of mass transport properties of these formations. The Queenston shale was found to have an average porosity of 0.066 ± 0.005 , and average iodide and tritium diffusion coefficients of $(1.2 \pm 0.3) \times 10^{-12}$ and $(1.1 \pm 0.3) \times 10^{-11}$ (m^2/s). The Cobourg limestone had an average porosity of 0.017 ± 0.003 , and average iodide and tritium diffusion coefficients of $(1.2 \pm 2.4) \times 10^{-12}$ and $(3.9 \pm 4.8) \times 10^{-12}$ (m^2/s). The average pore diameters of shale and limestone were 6.2 ± 0.9 nm and 7.7 ± 1.6 nm, respectively. The matrix permeability of these samples was very low, with average values of $(4.5 \pm 5) \times 10^{-21}$ (m^2) for Queenston shale and $(9.4 \pm 7.0) \times 10^{-22}$ (m^2) for Cobourg limestone. Porosity and pore geometry variation accounted for differences in diffusivity and permeability between shale and limestone. Leaching experiments to extract soluble salts indicated that the pore waters in Ordovician sediments are highly saline, with Total Dissolved Solid (TDS) values estimated to range from 180 to 270 g/L. These compositions are consistent with the compositions of groundwaters from wells within Ordovician-aged formations in southern Ontario.

TABLE OF CONTENTS

	<u>Page</u>
ABSTRACT	v
1. INTRODUCTION	1
2. METHODS.....	5
2.1 SAMPLE COLLECTION AND PRESERVATION.....	5
2.1.1 Recommended Sampling Methods	5
2.1.2 Archived Samples Used in this Study	6
2.2 POROSITY ESTIMATION BY WATER IMMERSION	8
2.2.1 Background	8
2.2.2 Modified Water Immersion Method for Sedimentary Rocks	9
2.3 MERCURY INTRUSION POROSIMETRY	13
2.4 THROUGH-DIFFUSION CELL MEASUREMENTS OF DIFFUSIVITY AND ROCK CAPACITY	16
2.4.1 Definitions of Diffusion Coefficients.....	16
2.4.2 Experimental Theory.....	18
2.4.3 Through-diffusion Cell Experiments for Sedimentary Rocks	20
2.5 RADIAL DIFFUSION EXPERIMENTS	23
2.6 PERMEABILITY ESTIMATION.....	25
2.7 ESTIMATION OF PORE FLUID COMPOSITION	27
3. RESULTS	29
3.1 POROSITY	29
3.2 MERCURY INTRUSION POROSIMETRY RESULTS.....	31
3.3 THROUGH-DIFFUSION CELL MEASUREMENTS	32
3.3.1 Effect of Sample Thickness	32
3.3.2 Stability of Shale Samples	34
3.3.3 Effective Diffusion Coefficients for Shales and Limestone	37
3.4 PERMEABILITY	40
3.5 PORE FLUID COMPOSITION.....	44
4. DISCUSSION	45
4.1 DIFFUSIVE PROPERTIES OF SEDIMENTARY ROCKS	45
4.2 SUGGESTIONS FOR FUTURE WORK.....	50
5. CONCLUSIONS	51
ACKNOWLEDGEMENTS.....	52
REFERENCES	53
APPENDIX A: LEACH DATA TO DETERMINE PORE WATER COMPOSITION.....	57

LIST OF TABLES

	<u>Page</u>
Table 1: Diffusion Parameters for Sedimentary Rocks from the Literature	2
Table 2: Porosity Values Derived from Queenston Shale	29
Table 3: Porosity Values Derived for Cobourg Limestone	30
Table 4: MIP Data for Queenston Shale	32
Table 5: MIP Data for Cobourg Limestone	32
Table 6: Sample Matrix for Diffusion Cell Experiments	37
Table 7: Iodide and Tritium Diffusion Parameters for Queenston Shale	38
Table 8: Iodide and Tritium Diffusion Parameters for Cobourg Limestone.....	39
Table 9: Permeability Measurements of Archived Core Samples	41
Table 10: Permeability Measurements of Fresh Queenston Shale Samples	42
Table 11: Pore Water Concentrations of Anions and Cations Leached From Queenston Shale	44
Table 12: Pore Water Concentrations of Anions and Cations Leached From Cobourg Limestone.....	45
Table 13: Compare Diffusion Coefficients and Porosities to Literature Values	46
Table 14: Average Parameter Values Affecting Mass Transport	47
Table 15: Compare Pore Water Compositions with Groundwater Compositions	49

LIST OF FIGURES

	<u>Page</u>
Figure 1: Core SI 2005-1, with Queenston Shale	7
Figure 2: Core DW-46 Cobourg (Lindsay) Limestone, with Marked Sample Locations	7
Figure 3: Examples of Queenston Shale Core Slices Showing Disintegration after Wetting ...	9
Figure 4: Queenston Shale Sample Mounted in a Diffusion Cell and Showing No Sample Disintegration after Wetting.....	9
Figure 5: Vacuum Cell for Saturating Rock Samples.....	10
Figure 6: Plastic Cups for Containing Rock Samples in Vacuum Cell	11
Figure 7: Schematic Diagram of Set-up for Determining Sample Volume	11
Figure 8: Example of Drying Curve to Determine the Water-saturated but Surface-dry Weight (Ws) for a Queenston Shale Sample	13
Figure 9: Penetrometer Stems Used to Hold Samples During MIP Analyses	14
Figure 10: Micromeritics Autopore #9220 Mercury Intrusion Porosimeter	15
Figure 11: Example of Tracer Mass Diffusion in a Through-diffusion Experiment	19
Figure 12: Schematic Diagram of a Laboratory Diffusion Cell	21
Figure 13: Diffusion Cell Loaded with Sample of Queenston Shale.....	22
Figure 14: Three Diffusion Experiments in Progress	23
Figure 15: Installing a Radial Diffusion Experiment	24
Figure 16: Rock Core Sample (shale) Enclosed by End Pieces to be Used in a Permeability Measurement	26
Figure 17: Rock Core Sample Coated with Silicon and Ready to be Loaded in Pressure Vessel for Permeability Measurement.....	26
Figure 18: HPRM Facility for Measuring Permeability	27
Figure 19: Shale Samples Being Leached to Determine Pore Fluid Composition	28
Figure 20: Example of Drying Curve (Core #4) to Determine the Dry Weight of Limestone Sample.....	30
Figure 21: Typical Pore Size Distributions for Shale and Limestone	31
Figure 22: Iodide Mass Diffusion Plots for Samples of Queenston Shale with Thicknesses of 5, 10, and 30 mm	33
Figure 23: Core Slice of Queenston Shale Immersed in 170 g/L KNO ₃ Showing a Parting Pattern Typical of Unconfined Samples Immersed in Water	34
Figure 24: Iodide Diffusion in a Shale Sample (REV 20 mm) Containing a Zone of Fast Transport	36
Figure 25: Tritium Diffusion in a Shale Sample (REV 20 mm) Containing a Zone of Fast Transport	36
Figure 26: Effect of Confining Pressure on Permeability (Perp = perpendicular to bedding; para = parallel) for Archived Samples (A) and Shale from Bruce Site (B).....	43

1. INTRODUCTION

A geoscientific assessment has been completed on the suitability of the Paleozoic sedimentary rock sequence occurring beneath southern Ontario to host a Deep Geologic Repository (DGR) for used nuclear fuel (Mazurek 2004). The assessment involved a review of international radioactive waste management programs in sedimentary media and a compilation of existing and publicly available geoscientific information for southern Ontario. Based on an initial assessment using simple criteria (existence of low hydraulic conductivity rock mass, formation depth below ground surface, formation thickness, and simple formation geometry), suitable bedrock formations were identified as the Middle/Upper Ordovician age (ca. 470 - 443 Ma) shales (Blue Mountain, Georgian Bay and Queenston Formations) and underlying limestones (Simcoe Group, i.e., the Gull River, Bobcaygeon, Verulam and Lindsay Formations). One of the important conclusions from this initial assessment is that these deeper subsurface formations contain stagnant water, and that solute transport was expected to be dominated by diffusion, even in those formations which have higher permeabilities. Mazurek (2004) indicated that future work to determine the suitability of Ordovician sediments to host a DGR should include the acquisition of formation specific data to support the quantification of solute transport retardation, such as mineralogy, porosity, diffusivity, ion exchange and sorption characteristics, pore-water composition and redox state.

The suitability of sedimentary formations as host rocks for the disposal of radioactive waste in deep geologic repositories is currently being assessed internationally. Radioactive waste management programs in Switzerland, France, Belgium, Spain and Japan are focused on clay-rich sedimentary rocks as potential host formations. However, direct measurements of porosity and diffusion coefficient values for shales and limestones from southern Ontario are limited in the published literature. Barone et al. (1990), reported porosity values of 0.102 to 0.114 and a CI effective diffusion coefficient (D_e) of $1.5 \times 10^{-11} \text{ m}^2/\text{s}$ for the upper Ordovician Queenston shale from southern Ontario (Burlington), taken from a depth of 11 to 12 m. Mazurek (2004, after Golder Associates 2003) reported porosity values of 0.005 to 0.03, and CI D_e values of 5×10^{-13} to $3 \times 10^{-12} \text{ m}^2/\text{s}$ for Gull River limestones.

Examples from the international literature of diffusion parameters determined for sedimentary rocks, including clay, argillite, limestone and sandstone are summarized in Table 1. Porosity values for sedimentary rock are one to two orders of magnitude higher than in crystalline igneous rocks, which typically have porosities between 0.002 and 0.003. Based on the limited data available, shales in southern Ontario appear to have porosities similar to Scotian Shelf shales, and many European argillite formations. Although in some cases sedimentary D_e values are similar to those determined for crystalline igneous rocks, often the sedimentary values are one to two orders of magnitude higher. This suggests that the experimental times to study diffusion in sedimentary rocks will be shorter than was required for Lac du Bonnet granite (Vilks et al. 2004). The reported CI D_e value for Queenston shale from southern Ontario is slightly higher than the CI and I D_e values reported for the Opalinus clay and other Canadian clays. In clay-rich rocks, diffusion parallel to bedding planes is reported to be higher than diffusion normal to bedding planes by a factor 2 to 5 (Van Loon and Soler 2004, Mazurek et al. 2003). The diffusion properties of limestone cover a broader range compared to clays and shales, which is not surprising given the range of rock textures that can be observed in limestones.

Table 1: Diffusion Parameters for Sedimentary Rocks from the Literature

Formation/Rock Type	Ref	Porosity	Method	D _e for			
				HTO	D _e for I	D _e for Cl	
Boom Clay - Mol	7	0.37		7.70E-11			⊥ bedding
Boom Clay - Mol	7			1.50E-10			bedding
Spanish Reference Clay	7	0.39		1.20E-10			⊥ bedding
Avonlea bentonite	8				3.0E-10		
Avonlea bentonite	9				3E-12 - 6E-11		
compacted bentonite	5	0.05 to 0.11	α I		5.3E-12 - 9.4E-12		
Lake Agassiz clay	8	0.32	fluid sat		5.7E-13		
Lake Agassiz clay	3	0.1	calc.		9.0E-12 - 5.3E-11		
Callovo-Oxfordian argillite	7	0.15		1.40E-11			⊥ bedding
Callovo-Oxfordian argillite	7			2.00E-11			bedding
Callovo-Oxfordian argillite, Andra URL	4	0.025 to 0.20	α HTO	2.6E-12 - 4.5E-11			
Couche Silteuse - argillite, France	7	0.08		1.00E-11			
Opalinus Clay - Benken	12	0.13 to 0.14	α HTO		4.5E-13 - 6.6E-13		
Opalinus Clay - Benken	12	0.06 to 0.08	α I	5.40E-12	6.6E-13	6.7E-13	⊥ bedding
Opalinus Clay - Benken	12	0.13 to 0.15	α HTO				
Opalinus Clay - Benken	12	0.045	α Cl	3.15E-11		3.4E-12	bedding
Opalinus Clay - Benken	12	0.14 to 0.17	α HTO				
Opalinus Clay - Mont Terri	12	0.08	α Cl		3.3E-12 - 4.8E-12		
Opalinus Clay - Mont Terri	12	0.08 to 0.11	α I	1.40E-11	4.8E-12	4.1E-12	⊥ bedding
Opalinus Clay - Mont Terri	12	0.15 to 0.17	α HTO				
Opalinus Clay - Mont Terri	12	0.082	α Cl	5.40E-11		1.6E-11	bedding
Opalinus Clay - Mont Terri	11	0.09 to 0.11	α HTO				
Opalinus Clay - Mont Terri	11	0.05	α Cl	1.2E-11 - 1.5E-11	3.2E-12 - 4.6E-12	4.0E-12 - 5.5E-12	⊥ bedding
Opalinus Clay - Benken	7	0.07 to 0.10	α I				
Opalinus Clay - Benken	7	0.124		1.00E-11			⊥ bedding
Opalinus Clay - Benken	7			5.00E-11			bedding
Opalinus Clay - Mont Terri	7	0.157		1.50E-11			⊥ bedding
Opalinus Clay - Mont Terri	7			6.30E-11			bedding
Opalinus Clay - Mont Terri	10	0.125 to 0.145	fluid loss	1.00E-11			in-situ bedding

Table 1: Concluded

Formation/Rock Type	Ref	Porosity	Method	D _e for HTO	D _e for I	D _e for Cl
Palfris Formation, Wellenberg shales from Scotian shelf	7	0.29		2.00E-12		⊥ bedding
Toarcian/Domerian argillite	6	0.015 to 0.12	fluid sat.			
Toarcian/Domerian argillite	7	0.1		4.00E-12		⊥ bedding
Toarcian/Domerian argillite	7			1.50E-11		bedding
Upper Ordovician Shales, S. Ontario	1	0.108	fluid sat.			1.5E-11
limestones	2	0.03 to 0.43	fluid sat.		6.8E-13-	2.9E-10
Oxfordian limestone - Andra URL	4	0.03 to 0.24	α I	2.6E-12- 1E-10		
sandstones	2	0.11 to 0.25	fluid sat.		1.7E-11 -	7.1E-11

α I Refers to porosity determined by iodide rock capacity

α Cl Refers to porosity determined by chloride rock capacity

α HTO Refers to porosity determined by tritium rock capacity

References:

- | | |
|------------------------------|-----------------------------|
| 1. Barone et al. 1990 | 7. Mazurek et al. 2003 |
| 2. Boving and Grathwohl 2001 | 8. Oscarson and Hume 1994 |
| 3. Choi et al. 1993 | 9. Oscarson et al. 1992 |
| 4. Descostes et al. 2004 | 10. Palut et al. 2003 |
| 5. Eriksen and Jansson 1996 | 11. Van Loon et al. 2003 |
| 6. Katsube et al. 1992 | 12. Van Loon and Soler 2004 |

Any comparison of the diffusion properties of tritium with those of anions (I, Cl) must take into consideration that tritium can access all water-containing connected porosity (because water contains hydrogen atoms). In contrast, anions may be excluded from a fraction of the total connected porosity as a result of repulsion by the dominantly negative charged mineral surfaces (anion exclusion). Consequently, tritium-derived porosities (from rock capacity factors) and tritium D_e values will often be higher than those determined using anions as tracers.

The current research was undertaken to develop and test laboratory protocols to measure bulk diffusive transport properties in sedimentary rocks, with an emphasis on shales and limestones. Experimental techniques for characterizing rock diffusion parameters for crystalline rock in were previously developed within the Deep Geologic Repository Technology Program (DGRTP) (e.g., Vilks et al. 1999, 2004). The approach to developing experimental procedures for sedimentary

rock was to build on this experience by comparing these methods to published work on the estimation of diffusion parameters in sedimentary rock (e.g. Boving and Grathwohl 2001, Descostes et al. 2004, Mazurek et al. 2003, Van Loon and Soler 2004). Sedimentary rocks have larger porosities, and different rock fabrics and mineralogy than crystalline rocks. Therefore, initial tests with samples of sedimentary rock (Queenston shale and Whirlpool sandstone) to estimate porosity and diffusivity were performed to determine whether the differences between sedimentary and igneous crystalline rocks may affect the application of experimental techniques previously used for igneous rocks, and to develop alternative techniques when necessary.

Initial experiments with shale samples focused on applying existing experimental procedures to measure diffusivity and porosity, to determine whether these samples would be subject to alteration caused by swelling or some other process. For example, tunnels built in shales and shaley rocks in Southern Ontario have shown evidence of stress-dependent long-term swelling deformation (Hawlder et al. 2005). Because shales are composed mostly of clay (illite), swelling may be induced by water migration or changes in water chemistry. The application of stress can also affect swelling (Hawlder et al. 2005). If swelling of shale samples occurs, steps need to be taken to control it, and/or to understand its effect on porosity and diffusivity.

Shales have a significantly higher porosity than crystalline rock, which might impact porosity estimation by the water immersion technique. A significant fraction of this porosity might include small constricted pore spaces associated with clay minerals. In this study it was determined that it is necessary to measure dry sample weight by oven drying, as recommended by Katsube et al. (1992), instead of drying under a vacuum at room temperature, as was done for granites (Vilks et al. 2004).

Sedimentary rocks often contain significant amounts of carbonates or sulphates as major rock forming minerals or as matrix and fracture filling cement. If the formation contains saline groundwaters, the pores of the rocks may contain saline pore fluids. In the diffusion experiments, the tracer fluid itself may result in changes in the porosity, pore structure, and/or connectivity if dissolution or precipitation of minerals occurs within the rock matrix as a result of interaction with the tracer fluid. In order to obtain more representative results the ionic strength and/or the chemical composition of solutions used in diffusion experiments can be adjusted to minimize rock-water interactions during the experiment.

As a result of the presence of sedimentary structures such as bedding planes, fossils, secondary porosity, etc., the Representative Elementary Volume (REV) of sedimentary rocks is likely different than granitic rocks. In this study, the effect of sample size on diffusivity measurements was assessed for shales by determining the variation of estimated diffusivity values with sample thickness.

This report describes the testing of laboratory procedures for estimating the porosity, diffusivity, permeability and pore water chemistry of sedimentary rocks. It recommends test protocols for characterizing the bulk diffusion parameters for sedimentary rocks, and it presents initial estimates of porosity, pore size, effective diffusivity, permeability and pore water chemistry determined using archived core samples from both the Queenston formation (shale) and from the Cobourg Formation (argillaceous limestone).

2. METHODS

2.1 SAMPLE COLLECTION AND PRESERVATION

The primary goal is to obtain and store representative rock samples without altering their porosity and pore geometry. The preservation of pore water chemistry is of interest, but is of secondary importance in diffusivity measurements, as long as chemical/biological processes do not lead to changes in porosity during sample storage. In general, the selection of sampling locations should consider the experimental objectives.

2.1.1 Recommended Sampling Methods

Sample size: In diffusion cell experiments, the diameter of the sample core determines the surface area through which tracer can diffuse. Although cores with diameters as small as 22 mm have been successfully used for diorite samples from Äspö, the small surface areas have contributed to significantly lower diffusive fluxes, resulting in very long times to achieve steady-state diffusion. The 47 mm diameter cores used for samples of Lac du Bonnet granite and granodiorite produced much faster diffusion rates. Therefore, it is recommended that samples of sedimentary rock be drilled to produce cores with diameters of 47 mm and larger. If radial diffusion experiments are to be performed, core sections with a 200 to 300 mm diameter would be required, but are not commonly drilled.

The sample length required to achieve a REV depends upon the texture of the sample being studied. For example, coarse grained rocks require a longer sample length than fine grained rocks because larger grains produce a greater variability in pore geometry in a given rock volume. Increasing sample size incorporates this variability into the bulk diffusivity measurement. In sedimentary rocks, samples with fossils may require special attention when evaluating the REV, because void spaces created by fossils may produce fast diffusion paths. Typically, diffusion measurements on shales or clays have used sample thickness' of 10 mm. Tests using sample thickness' of 5, 10, 20, and 30 mm should be performed to determine whether the 10 mm thickness is appropriate for the lithology being investigated. The need to evaluate REV would be determined by variations in lithology (e.g. from fossiliferous to fine-grained) and the presence of secondary porosity created by diagenesis or tectonic deformation.

Drilling procedures: Standard drilling procedures can be used for collecting core samples for diffusion experiments. The intent is to recover core as quickly as possible with minimal thermal effects on the sample. Martin and Stimpson (1994) found that stress-induced damage in samples of granite becomes significant below depths of about 200 m. They argued that the stress-induced damage occurred during the drilling process, at which time the 3-dimensional stress concentrations at the face of the drill bit magnified the effects of the in-situ stress conditions by a factor of 2, enough to produce microcracks. The amount of stress induced damage was not related to core diameter, or to poor quality rock sampling procedures.

Because knowledge of pore fluid compositions is valuable for formulating tracer and eluant solutions, and for better understanding diffusivity under in-situ conditions, it is important to understand the effect of drilling on pore fluid chemistry. Because diffusivity in Ordovician shales and limestones is assumed to be low, drilling fluids are not expected to exchange

significantly with pore fluids over the 2 to 8 hour time period required to recover a 1 m core section. However, to confirm that assumption it might be useful to add uranine or another distinctive tracer to the drilling fluid.

Sample preservation: After drilling, it is important to store sample core in such a way as to minimize any further changes to the rock structure and porosity. Over long time periods it is best to store rock samples in core boxes as intact cores (~ 1 m sections). Smaller sub-samples for diffusivity, porosity and permeability measurements are cut shortly before use. The porosity of thin (10 mm) slices of granite core was found to increase by 37 to 46 percent during a two year storage time, whereas intact core showed no effects from aging (Vilks et al. 1999). It is not known whether a similar alteration process would affect sedimentary rocks. If sample cores are to be drilled specifically for diffusion and pore water studies, then the pore fluid content must be preserved by minimizing sample drying. Although drying is likely to leave the salt content behind, the drying process could induce some irreversible reactions that will prevent the total recovery of pore fluid salts during the leaching process. To minimize drying, one possible preservation procedure involves wrapping fresh core in multiple layers of thin plastic immediately after being cut. The cores are then placed in plastic tubes, and the ends are sealed. For further protection, the plastic tubes are placed in a plastic sleeve that is heat-sealed. Other examples of preservation methods include wrapping fresh core with saran wrap, covered with wet tissue for Queenston shale (Barone et al. 1990), and wrapping shale in kerosene-saturated paper, covered with aluminum foil (Fam and Dusseault 1998).

2.1.2 Archived Samples Used in this Study

In the current study, rock samples were obtained from archived cores that had been subject to routine handling procedures, without any attempt to prevent the drying of pore fluids.

Samples of Upper Ordovician Queenston shale were obtained from core SI 2005-1 (Figure 1), which was drilled during February 2005 in Niagara Falls, Ontario. Prior to sampling the core was stored in standard wooden core boxes, with no protection against drying. The core was in good condition, allowing selection of large pieces for diffusion studies. The core diameter was 63.3 mm. The Whirlpool sandstone was located at a core depth of 72.4 m, while Queenston shale samples were taken at depths ranging from 73.5 to 110.5 m. The Queenston shale is situated in the westernmost part of the Taconic clastic wedge of eastern North America, and was formed in a depositional environment that consisted of a wide, shallow, prograding shore that was probably affected by tides, recurring storms, drainage channels, and temporary sub aerial exposure (Brogly et al. 1998).

Samples of Upper Ordovician Cobourg (Lindsay) limestone (Figure 2) were taken from core DW-46 (Box #5), which had been drilled in 1978 as part of geotechnical investigations and stored in an unheated core shed. As with the Queenston Formation core from Niagara Falls, no steps had been taken to preserve moisture content within the core or to prevent exposure to freeze-thaw cycles. Three core samples were selected and shipped by OPG for characterization of diffusion properties. The core diameter is 54.5 m, and the sample depths ranged from 36.4 to 55.9 m. The Cobourg limestone is a nearshore deposit containing calcareous mud and layers of fossils reworked by storm wave action. A visual inspection of hand specimens suggests that sedimentary structures could influence the direction of diffusive mass transport.



Queenston Shale

Figure 1: Core SI 2005-1, with Queenston Shale

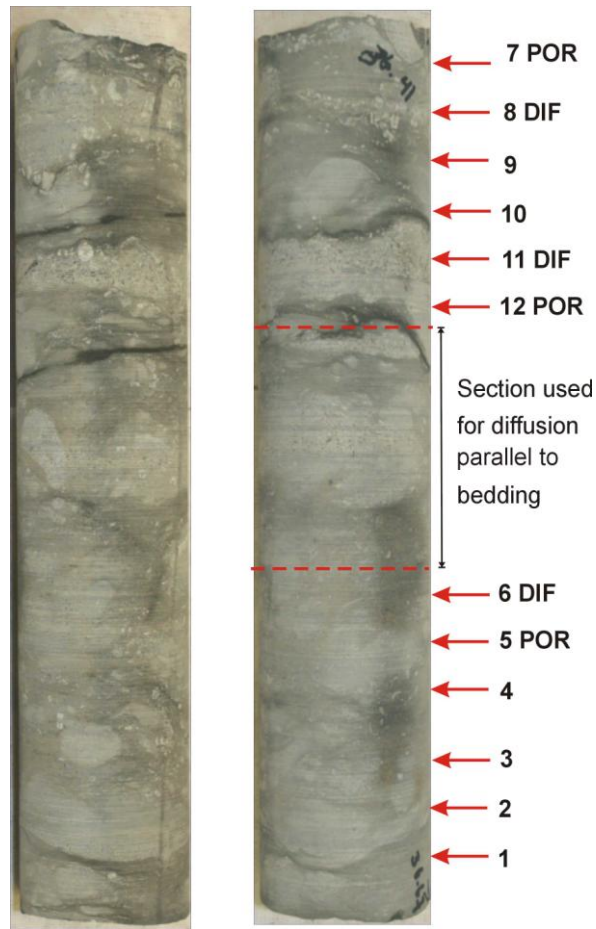


Figure 2: Core DW-46 Cobourg (Lindsay) Limestone, with Marked Sample Locations

2.2 POROSITY ESTIMATION BY WATER IMMERSION

2.2.1 Background

All methods developed for estimating connected porosity involve filling the connected voids with a quantifiable substance or tracer. The usefulness of a given method depends on the ability of the tracer to penetrate all relevant pore space, and on the ability to quantify the tracer. The principal method used in the current study is the water immersion technique. Examples of other methods include (1) helium porosity (Valkiainen et al. 1995), which involves the filling of rock pore spaces with helium gas under controlled conditions (Dorsch 1997), (2) mercury porosimetry (Barone et al. 1990) for porosities greater than 1%, and (3) leaching tests using tritium (HTO) or helium (Olin et al. 1997).

The water immersion technique (also referred to as fluid saturation), refined by Melnyk and Skeet (1986) for rocks with porosities less than 5 %, has been widely used in many studies with crystalline rocks (Vilks et al. 2004). An inter-laboratory comparison has indicated that the water immersion technique is one of the most reliable techniques for rocks of low porosity (Rasilainen et al. 1996). The water immersion technique is also applied to sedimentary rocks (API 1960, Katsube et al. 1992). In the water immersion technique, a rock sample is saturated with distilled de-aerated water under vacuum and then the weight of water in pore spaces is determined by monitoring the weight of the rock sample while it dries. Melnyk and Skeet 1986, determined the actual dry weight of the sample by drying it under vacuum until a constant weight was achieved. They avoided heating the sample because of concerns that heating to temperatures as low as 70°C could cause significant damage to the rock porosity. However, in an extensive evaluation of porosity estimation methodology on shales from the Scotian Shelf, Katsube et al. 1992, found that vacuum drying was not sufficient to remove all water from pore spaces. They found that the optimum method for determining dry weight of these shales was to heat the sample to 105°C or 116°C, as a last step in the porosity measurement process. Heating to this temperature is sufficient to remove water from open pore spaces, but does not remove the water adsorbed to mineral surfaces and found in the interlayer spaces of clay minerals. A higher temperature range of 200 to 260°C is required for removing the more strongly held water. Repeated measurements produced consistent porosities, and any progressive porosity increases could be attributed to damage by sample handling. The samples, which showed the most change with repeated measurements, were those with a high content of illite, smectite or organic matter.

A series of preliminary experiments were carried out with samples of Queenston shale to estimate porosity using the method of Melnyk and Skeet 1986, and procedures used by Katsube et al. 1992, for shales from the Scotian Shelf. Experimental results showed that the archived Queenston shale samples have properties that render them unsuitable for analyses using the method of Melnyk and Skeet (1986). Archived samples of the Queenston shale were found to be prone to disintegrate after being wetted (Figure 3), making subsequent sample handling more difficult compared to crystalline rock or sandstone. Clay-bearing rocks, such as shales, are known to swell or disintegrate when exposed to atmospheric wetting and drying (Franklin and Dusseault, 1989). It should be noted that the Queenston shale samples did not show this behaviour when mounted in diffusion cell sample holders (Figure 4). The water immersion method has been modified to account for the larger porosity and the fragile nature of the Queenston shale samples, as described in the following section.



Figure 3: Examples of Queenston Shale Core Slices Showing Disintegration after Wetting

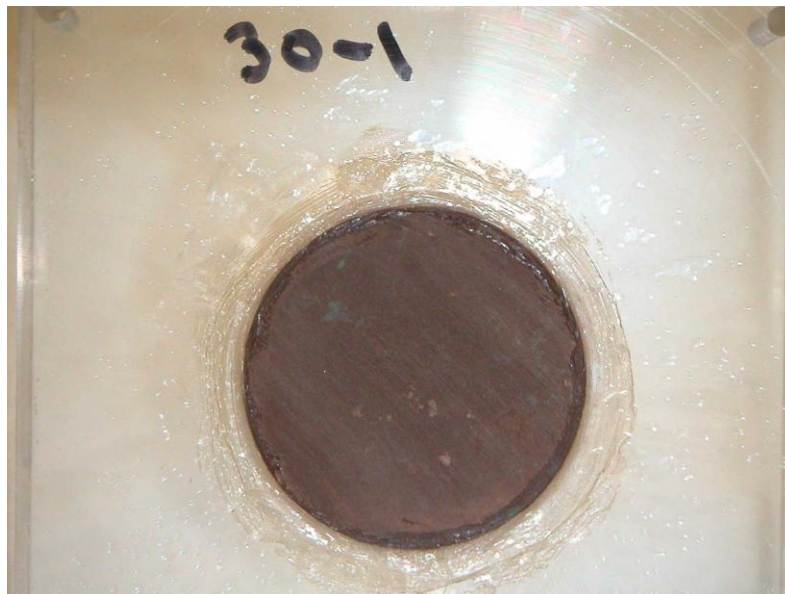


Figure 4: Queenston Shale Sample Mounted in a Diffusion Cell and Showing No Sample Disintegration after Wetting

2.2.2 Modified Water Immersion Method for Sedimentary Rocks

The main differences in the modified method for estimating porosity of shales are that the sample dry weight is determined by oven drying instead of vacuum drying, and sample

saturation and subsequent handling have been modified to account for the fragile nature of shale samples.

The initial mass of a rock sample used for porosity estimation is between 20 and 70 g. In the case of the Queenston shale samples used in the preliminary experiments, the samples consisted of 45 mm diameter core cut into slices with thickness' ranging from 5 mm to 30 mm. Core slices are cut with a water-cooled diamond saw. Each sample is washed with deionized water before use. In the method used for crystalline rocks, the samples were also sonified during the washing procedure to assist in the removal of loose particles. However, due to the fragile nature of the Queenston shale after wetting, the sonification step was eliminated. While the removal of loose particles was thought to be important for crystalline rocks because they had very low porosities around 0.3 percent, the impact of loose material would have a minor affect on sedimentary rocks that have higher porosities with water contents that are easier to determine.

Before saturating the rock samples with water, they are placed in a vacuum cell and evacuated for at least 24 hours (Figure 5). Within the vacuum cell, each sample is contained in a separate plastic cup that has holes cut in the bottom to allow access to water (Figure 6), and which keeps the sample pieces together if the sample disintegrates. During this time, 500 mL of demineralised water are degassed under vacuum. Once the initial drying stage is complete, the vacuum cell containing the rock samples is isolated from the vacuum pump, and degassed water is slowly allowed to enter the vacuum cell and completely immerse the rock samples. The samples are kept under water for at least 24 hours to allow full water penetration of the pore spaces. Queenston shale samples were likely to break apart while sitting in the water. In this case, the larger usable pieces are selected for continuation of the porosity measurements. The samples are maintained in a wet condition until their water saturated weight is determined.

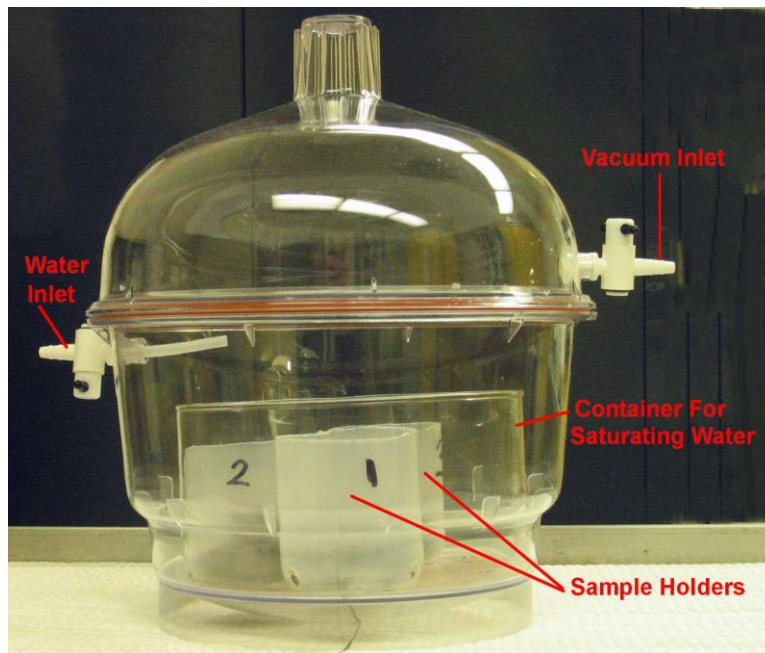


Figure 5: Vacuum Cell for Saturating Rock Samples



Figure 6: Plastic Cups for Containing Rock Samples in Vacuum Cell

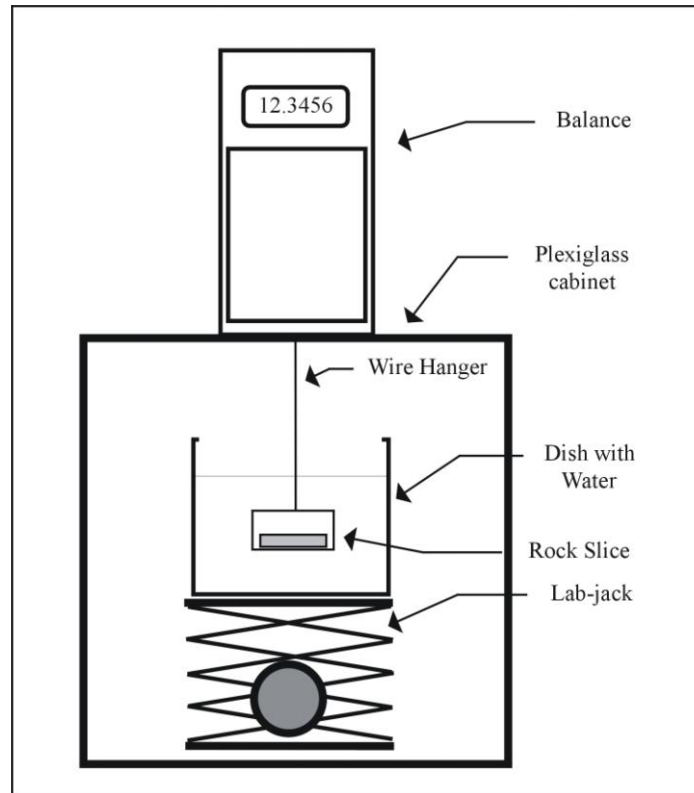


Figure 7: Schematic Diagram of Set-up for Determining Sample Volume

The rock sample volume (V_s) and the water-saturated but surface-dry weight (W_s) are determined in the next two sequential steps. After running a daily balance calibration check, a large dish filled with demineralised water is positioned under a balance (Figure 7) so that the under-the-balance hanger is immersed under water exactly to a marked level. After ensuring that no bubbles are clinging to the surface of the hanger, the balance is tarred. The lab-jack holding the water dish is lowered to remove the hanger from the water, and the largest piece(s) of sample are placed onto the hanger. The lab-jack is then raised so that the hanger is immersed exactly to the mark. After ensuring that there are no clinging air bubbles, the weight (W_{vs}) is recorded. The lab-jack is raised and lowered at least five times to determine the repeatability of the measured weight.

Because the rock sample contains water within its pores, as well as on the surface, it is necessary to eliminate the surface water, which may produce an erroneously high porosity if included. To determine the water-saturated but surface-dry weight (W_s), the water bath is lowered out of the way after the sample volume has been determined. After removing the sample, the hanger is dried and the balance is tarred. Excess water is gently wiped from the sample with a damp lint free tissue and the sample is replaced on the under-the-balance hanger. The sample weight is monitored while its surface dries using the Collect program to accumulate the weight loss data from the balance until the weight loss is small (<0.0005 g) or constant. A one hour drying time is usually sufficient. An example of a weight loss versus time curve is given in Figure 8. In the initial stage, weight loss is due mainly to evaporation from the sample surface. As the surface begins to dry, pore water starts moving toward the surface and contributes to the overall weight loss. When the sample is completely dry the weight loss represents only pore water. The sample weight (W_s) representing the point at which the surface is dry and the sample is still totally saturated is given by the intersection of the two lines representing drying from only the surface and drying only from pore spaces (Figure 8).

The dry weight (W_D) of the sample is determined by heating the rock samples in an oven at 105°C (after Katsube et al. 1992) for about 48 hours to remove all water from pore spaces. After heating, the rock samples are removed from the oven and left at atmospheric conditions for one hour. The samples are then repeatedly weighed until a constant weight (± 0.0005 grams) is obtained.

The sample porosity is calculated as follows:

W_D	Dry weight	
W_s	Water-saturated surface-dry weight	
W_{vs}	Water saturated submerged weight	
V_s	Sample Volume	
V_w	Volume of water in rock sample pores	
ρ_{H_2O}	Density of water at room temperature (22°) = 0.99777 g/cc	
ε	Porosity	
$V_s =$	$(W_s - W_{vs})/\rho_{H_2O}$	(1)
$V_w =$	$(W_s - W_D)/\rho_{H_2O}$	(2)
$\varepsilon =$	V_w/V_s	(3)

Note that this method assumes that the rock samples are fully saturated after 24 hours. Also, the drying process may not eliminate water adsorbed to mineral surfaces, which might be a factor in clay-rich rocks that have a high specific surface area. Also, rocks that originally

contained high salinity pore fluids will contain precipitated salts. These salts will dissolve when the rock is saturated with deionized water, producing a high density pore fluid. This higher density is not a factor in determining the volume of water that is evaporated from the rock because the salts are left behind. However, since the salts take up pore space the amount of water released during drying may underestimate the total connected porosity. For example, a simple gravimetric test shows that the water content in a 100 mL volumetric flask is 8.9 percent lower when the NaCl concentration is 250 g/L, compared to deionized water.

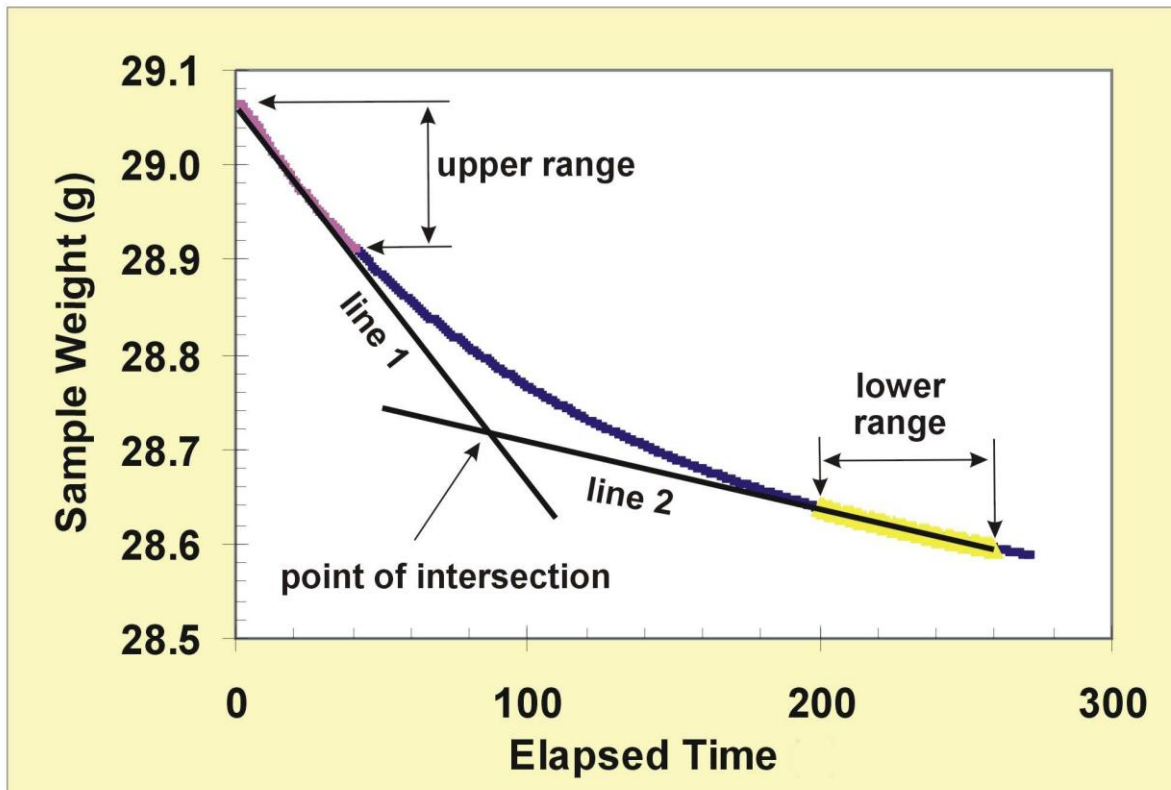


Figure 8: Example of Drying Curve to Determine the Water-saturated but Surface-dry Weight (W_s) for a Queenston Shale Sample

2.3 MERCURY INTRUSION POROSIMETRY

Mercury Intrusion Porosimetry (MIP) is a technique used to measure pore structure, as defined by a pore size distribution, in a variety of solid materials with pore diameters ranging from 3 nm to over 100 μm . Pore size and volume are determined by submerging the sample using a confined quantity of mercury, and then increasing the pressure of the mercury hydraulically. The detection of the free mercury diminution in the penetrometer stem (Figure 9) is based on a capacitance system and is equal to the mercury filling the pores. As the applied pressure is increased the total amount of intruded mercury increases as the mercury is forced into smaller and smaller pores. Determination of the pore size by mercury penetration is based on the behavior of non-wetting liquids in capillaries. A liquid cannot spontaneously enter a small pore

which has a wetting angle of more than 90 degrees because of the surface tension (capillary depression). However this resistance may be overcome by exerting a certain external pressure. In the derivation of pore size from exerted pressure, it is assumed that pores are cylindrical.

Samples of sandstone, shale and limestone were analyzed using a Micromeritics Autopore #9220 Mercury Intrusion Porosimeter (Figure 10). Before use, instrument calibration is checked, using Micromeritics Silica-Alumina Reference material P/N 004-16822-00, available from FOLIO Instruments INC. 159 Place Frontenac, Suite 1, Pointe Claire, Que. H9R 4Z7.



Figure 9: Penetrometer Stems Used to Hold Samples During MIP Analyses



Figure 10: Micromeritics Autopore #9220 Mercury Intrusion Porosimeter

Before analysis, samples must be dried to remove excess moisture, typically by placing in an oven at 95 degrees Celsius for 24 hours. After weighing, the sample is placed in a previously weighed penetrometer stem. The penetrometer is placed in a low pressure port on the porosimeter. The penetrometer is evacuated to 50 micrometers of mercury for a specified time period. Liquid mercury then automatically fills the penetrometer and surrounds the sample. The pressure placed on the mercury and sample is slowly increased to the crossover pressure (approximately 200 kPa). The computer controls the pressure steps and records the incremental intrusion. After completing this low pressure test, the penetrometer is removed, cleaned of any loose dirt, grease or mercury, and then weighed. The penetrometer is then placed into the high-pressure chamber and de-aired. The high-pressure test is started by increasing the pressure in a series of pre-defined steps up to 414 MPa (60,000 psi) and then decreasing it back down to 200 kPa (30 psi). The computer controls this operation, keeping track of the mercury intrusion at each pressure step. The computer calculates the pore size distribution, prints the data and also saves it to disk.

2.4 THROUGH-DIFFUSION CELL MEASUREMENTS OF DIFFUSIVITY AND ROCK CAPACITY

2.4.1 Definitions of Diffusion Coefficients

Diffusivity is a measure of the ability of a species to move through a medium under the influence of its concentration gradient. Diffusivity is quantified as a diffusion coefficient, D . Diffusivity can be measured under steady-state or transient conditions, and each has its advantages and area of applicability.

The processes of diffusion are described by Fick's first and second laws. In generalized situations, such as the conduction of heat in a solid, or the diffusion of species in a single phase medium such as water, Fick's first law states that the mass of a diffusing substance passing through a given cross section per unit time is proportional to the concentration gradient. In one dimension:

$$J = -D \cdot \frac{\partial C}{\partial x} \quad (4)$$

where

J is the mass flux, [mol/m²sec],
 D is the diffusion coefficient [m²/s],
 C is the species concentration [mol/m³], and
 $\partial C/\partial x$ is the concentration gradient;

Fick's second law is more general, and relates concentration with both space and time. In one dimension:

$$\frac{\partial C}{\partial t} = D \cdot \frac{\partial^2 C}{\partial x^2} \quad (5)$$

When evaluating diffusion through a fluid in a two phase system such as groundwater in a porous rock, it becomes necessary to modify Fick's laws, to account for the fact that the water only occupies a fraction of the total volume occupied by the rock. The modification is applied by redefining the diffusion coefficient (D) to include factors such as the porosity and the pore geometry, which is defined by a combination of tortuosity and constrictivity.

The diffusion coefficients that are used in Eqs. 4 and 5 to describe diffusivity in heterogeneous media have been defined to account for various combinations of the effects of porosity, tortuosity and constrictivity. The type of diffusion coefficient used depends on the particular application.

Because species diffuse through water in pore spaces, all diffusion coefficients applied to heterogeneous media can be related to free water diffusion coefficients (D_w). Free water diffusion coefficients have been measured for numerous cations and ions. Values of free water diffusion coefficients vary between 1.03×10^{-9} and 9.59×10^{-9} m²/s (e.g., Harvey 1996).

For certain applications, diffusion may be considered as a function of species concentration only in pore water. For example, this may be useful if diffusion data is available in the form of a diffusion profile, which shows changes in a species pore water concentration as a function of distance (e.g., Gimmi and Waber 2004). Diffusion in pore water is commonly described with a pore water diffusion coefficient, which accounts for the effects of tortuosity (τ) and constrictivity (δ) within connected pore spaces. This type of diffusion coefficient may be used as one of the input parameters in certain computer models that have porosity and diffusion as separate input parameters. The pore water diffusion coefficient (D_p) is defined as follows (Ohlsson and Neretnieks 1995):

$$D_p = \frac{D_w \delta}{\tau^2} \quad (6)$$

Diffusion can also be treated by considering a volume of rock as a whole. In this case, the connected porosity must be included in the calculation of the diffusive flux to account for the small volume of connected pore space compared to the volume of the whole rock. The effective or empirical diffusion coefficient (D_e) is commonly used to describe diffusive fluxes. Some authors (Bradbury et al. 1982) have also referred to this as the intrinsic diffusion coefficient (D_i). The effective diffusion coefficient is defined as (Choi and Oscarson 1996, Skagius and Neretnieks 1982, and Ohlsson and Neretnieks 1995):

$$D_e = \frac{D_w \delta \varepsilon_t}{\tau^2} \quad (7)$$

The through-transport porosity (ε_t) determines the diffusive flux through rock when steady state has been achieved. However, the storage capacity of the rock must also be considered. The storage capacity results from the dead end porosity (ε_d), and sorption for those species which are likely to adsorb onto mineral surfaces. The storage capacity is quantified by the rock capacity factor (α), which has been defined as (Bradbury and Green 1985):

$$\alpha = \varepsilon_c + \rho \cdot k_d \quad (8)$$

where ρ is the bulk density of the rock, k_d is the sorption coefficient, and the total connected porosity (ε_c) is given by:

$$\varepsilon_c = \varepsilon_t + \varepsilon_d \quad (9)$$

The rock capacity term can be incorporated into Fick's second law to describe concentration variation with space and time within a rock.

$$\frac{\partial C}{\partial t} = \frac{D_e}{\alpha} \frac{\partial^2 c}{\partial x^2} \quad (10)$$

The apparent diffusion coefficient (D_a) has been defined as (Bradbury and Green 1985, Choi and Oscarson 1996, Oscarson and Hume 1994 and Ohlsson and Neretnieks 1995):

$$D_a = \frac{D_e}{\alpha} = \frac{D_p \varepsilon_t}{(\varepsilon_c + \rho k_d)} \quad (11)$$

In the case of a nonsorbing tracer, such as iodide, the rock capacity term (α) is equal to the total connected porosity (ε_c). If the transport porosity (ε_t) is the same as the ε_c , the apparent diffusion coefficient for the nonsorbing tracer will be the same as the pore water diffusion coefficient (D_p).

The constrictivity (δ) and tortuosity (τ) are difficult, if not impossible, to determine separately by experimental means. Because of the difficulty in separating δ and τ , the term 'tortuosity' is often found in experimental work to have been used to describe the quantity $\tau / \sqrt{\delta}$. Melnyk and Skeet (1987) and Katsube et al. (1986) referred to the quantity $\tau / \sqrt{\delta}$ as an 'effective tortuosity' and define it as:

$$\tau_D^2 = \frac{\tau^2}{\delta} \quad (12)$$

The effective tortuosity values can be calculated from measured values of effective diffusion coefficients and estimated values of transport porosity, using Eq. 7, and assuming that ε_t and ε_c are identical. Effective tortuosity values may vary depending upon the tracer because the porosity used for diffusion may vary from one tracer to another. The porosity value used in Eq. 7 could be derived from water immersion or from diffusion experiments. Unless stated otherwise, effective tortuosities in this report were calculated using either measured or average values of porosity estimated by water immersion.

In this report the convention for reporting effective tortuosity focuses on the increased path length a solute must diffuse. By this convention the diffusion coefficient is reduced by effective tortuosity values greater than one. In the other commonly used convention for reporting tortuosity, the focus is on reporting tortuosity as a value by which the diffusion coefficient is reduced. By this convention the combined effects of tortuosity and constrictivity are reported as values of δ/τ^2 , with the diffusion coefficient being reduced by tortuosity values less than one.

2.4.2 Experimental Theory

In through-diffusion cell experiments, a rock sample is positioned between two solution reservoirs of equal hydraulic head. A concentration gradient is then established across the rock sample by addition of a tracer to one of the reservoirs. Once the system has reached a steady-state, the flux of tracer across the sample is measured and the effective diffusion coefficient of the tracer in the rock sample is determined. Vilks et al. (1999) have described a method used to estimate diffusion parameters from laboratory experiments on crystalline rocks, which is based on the work of Cramer et al. (1997), Bradbury et al. (1982), Wadden and Katsube (1982), Skagius and Neretnieks (1982), and Katsube et al. (1986). Following the initial breakthrough of tracer, the amount of tracer diffusing through the sample into the elution reservoir eventually reaches a steady-state, provided that the physical properties of the rock remain constant during the diffusion experiment (Figure 11). The mass of tracer (M_t) diffusing

through the sample under steady-state conditions at time (t) is described by the following equation:

$$M_t = D_e(C_o A/L) t - \alpha(ALC_o/6) \quad (13)$$

where

- D_e = effective diffusion coefficient for a given tracer in the rock sample,
- A = surface area through which the tracer diffuses,
- L = diffusion path length (i.e., thickness of rock sample),
- C_o = concentration of a given tracer in the tracer reservoir, and
- α = rock capacity factor

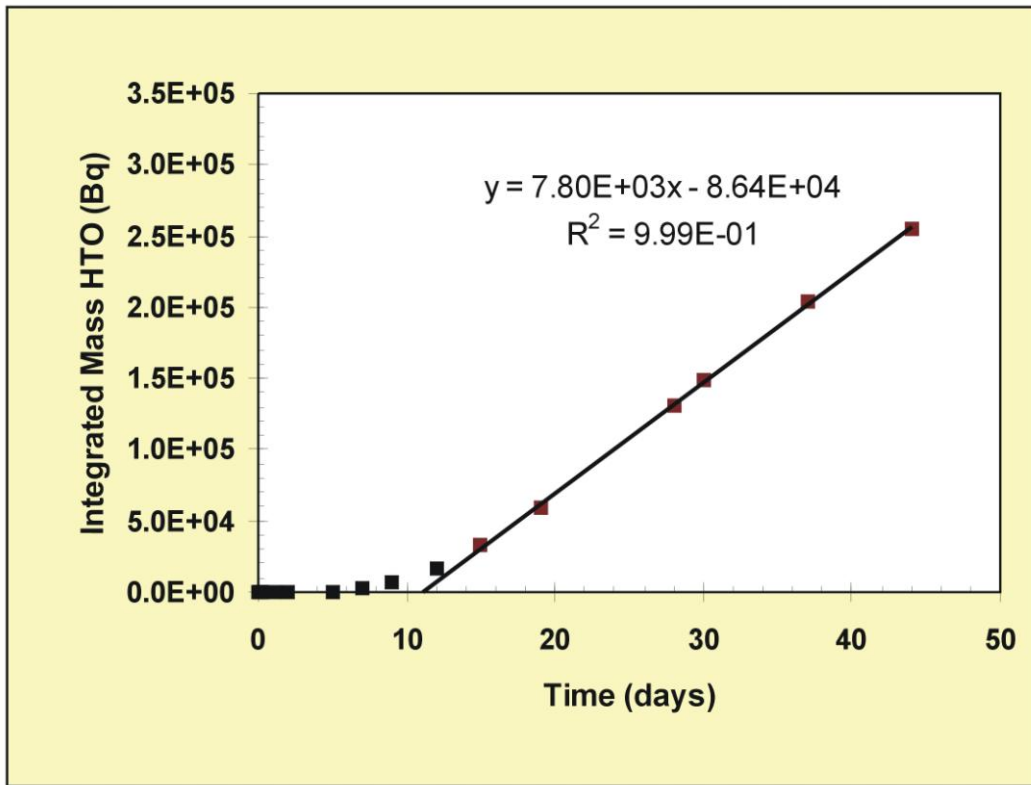


Figure 11: Example of Tracer Mass Diffusion in a Through-diffusion Experiment

When steady-state has been achieved a plot of M_t versus time will produce a straight line with a slope:

$$\text{Slope} = D_e(C_o A/L) \quad (14)$$

and an intercept:

$$\text{Intercept} = - \alpha(ALC_o/6) \quad (15)$$

Because C_o , A and L are known, the slope of the line can be used to calculate D_e . The intercept of the straight line can be used to calculate the dimensionless rock capacity factor (α), which represents the amount of tracer retained in the rock sample before steady-state is achieved. The magnitude of α depends upon the total connected porosity accessed by the tracer (ϵ_c) and on the amount of tracer that is adsorbed by the rock sample. Therefore, D_e and α are the basic parameters that can be estimated from through-diffusion data, without additional assumptions.

The error associated with estimated values of D_e is estimated from the uncertainty in the diffusive flux, which is obtained from the slope of the linear portion of the M_t versus time plot. This uncertainty is calculated from linear regression analysis. The error associated with values of rock capacity determined from diffusion experiments can also be estimated from the uncertainty of the intercept of the M_t versus time plots using linear regression analysis.

Through-diffusion type cells have been commonly used for crystalline rock samples, as well as for limestone and sandstone samples (Boving and Grathwohl 2001). If sample integrity is of concern, stainless steel filters may be used to separate the sample from the tracer and elution reservoirs. For example, these filters were employed for Oxfordian limestone and Callovo-Oxfordian argillite samples by Descostes et al. 2004, and for insuring the stability of compacted bentonite (Eriksen and Jansson 1996, Wold and Eriksen 2000). The diffusion and sorption properties of the stainless steel filters must be considered when interpreting the experimental results. If samples of compacted bentonite or shale, for example, are not fully saturated with water before being mounted in the diffusion cell, they may develop a swelling pressure upon saturation. Stainless steel diffusion cells have been designed to contain this swelling pressure (Sawatsky and Oscarson 1991, Choi et al. 1993). Diffusion cells used for natural clay samples have also been modified to allow for the application of a uniaxial stress to the clay sample by applying a known torque to the diffusion cell (Van Loon et al. 2003). Because through-diffusion experiments require long times to reach steady-state, it is advantageous to run several samples in parallel.

2.4.3 Through-diffusion Cell Experiments for Sedimentary Rocks

Laboratory diffusion experiments are performed using the diffusion cell schematically illustrated in Figure 12. The diffusion cell can hold a rock sample with diameter between 47 and 85 mm and a length of 5 to 60 mm. The sample is mounted within the diffusion cell sample holder using silicon cement (Figure 4 and Figure 13). In order to ensure that the sample is fully saturated before starting the diffusion experiment, the diffusion cell is filled with tracer-free eluant solution, which is allowed to penetrate the sample for several days. During this step the water level in the tracer reservoir is about 1 cm higher than in the elution reservoir to produce a hydraulic gradient to help force water into the sample. The diffusion experiment is initiated by replacing the tracer-free solution in the 1 L tracer reservoir with actual tracer and ensuring that the water level in the elution reservoir matches that in the tracer reservoir. Both reservoirs are open to atmospheric pressure. The elution reservoir is sampled to determine tracer diffusion through the rock sample. With each sampling, the volume of sampled solution is replaced by tracer-free eluant to maintain the height of solution in the elution reservoir at the same level as in the tracer reservoir. If tracer diffusion through the sample is very slow and the tracer concentration in the elution reservoir is less than 0.1 percent of that in the tracer reservoir, the elution reservoir is sampled on a periodic basis. However, if the diffusion process is likely to be faster, the elution reservoir is continuously sampled with a fraction collector to ensure that

tracer concentrations in the elution reservoir do not become too high, thereby reducing the tracer concentration gradient across the sample. The tracer concentration in the elution reservoir is kept low because of the continuous flushing with tracer-free eluant. As tracers diffuse through the rock sample, eventually a steady-state diffusive flux across the sample is achieved. The data characterizing the evolution of tracer concentrations in the elution reservoir to a steady-state, are used to calculate the rock capacity factor and effective diffusion coefficient of the rock sample (Vilks et al. 2004).

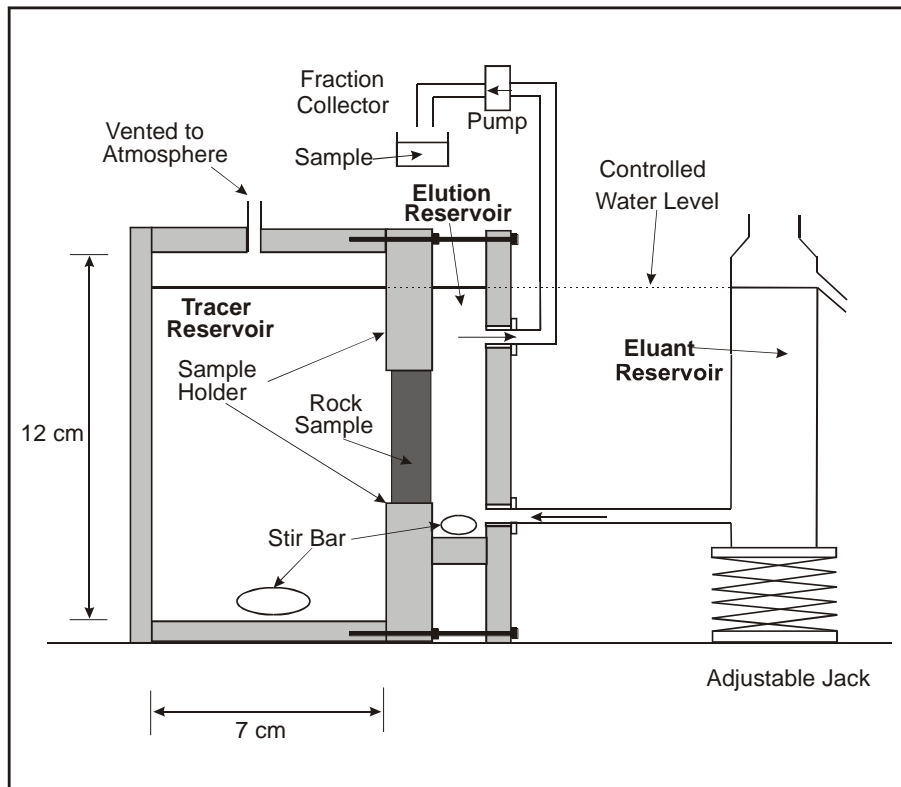


Figure 12: Schematic Diagram of a Laboratory Diffusion Cell

The conservative tracers used in these experiments are tritium to characterize diffusivity within all porosity accessible to water, and iodide to define diffusion in porosity readily accessible to anions. Uranine and Li are used as easily detectable, weakly sorbing tracers. As a result of the high clay content of the shales, significant retardation of uranine and Li in the shales is expected. The actual tracer solutions used in the initial experiments contained 9.1 g/L NaI, 6.9 g/L LiNO₃, 1.0 g/L uranine, and 1.3 x 10⁸ Bq/L tritium. The eluant solutions contained 17.0 g/L of KNO₃ to closely match the ionic strength and density of the tracer solutions to minimize density gradients and osmotic effects.

A final set of diffusion experiments was performed using solutions formulated to more closely match pore water compositions in shales and limestone. An estimation of the pore water compositions has been made in this initial study using simple leaching experiments (see Section 2.7). The intent of using solutions that closely match pore fluids was to minimize changes to porosity resulting from water rock interactions, and to measure diffusion under

conditions of high ionic strength closely matching in-situ conditions. The tracers used in these experiments were KI (166 g/L) and tritium (1.3×10^8 Bq/L). In addition to the iodide and tritium, the tracer solutions used for limestone contained 12 g/L NaCl, 11 g/L KCl, 33 g/L CaCl_2 , and 17 g/L MgCl_2 , while the tracer solution for shale contained 117 g/L NaCl and 7 g/L CaSO_4 . The tracer solutions used in this experiment were identical to the compositions used by the University of New Brunswick to study iodide diffusion through identical shale and limestone samples to facilitate a comparison of the bulk rock diffusion properties determined in this experiment to those measured for similar core samples using a newly-developed X-ray Radiography method at the University of New Brunswick. The eluant used in these experiments contained NaCl with concentrations intended to match the TDS of eluant solutions used by the University of New Brunswick.

Figure 14 shows a series of diffusion cell experiments underway. The tubing attached to each tracer reservoir is connected to a flask open to the atmosphere. This arrangement prevents evaporative loss from the tracer reservoirs while ensuring that each tracer reservoir is subject to the same fluctuations in atmospheric pressure experienced by the elution reservoirs. Note that in this particular experimental configuration, the elution reservoirs are not being continuously sampled by a fraction collector.

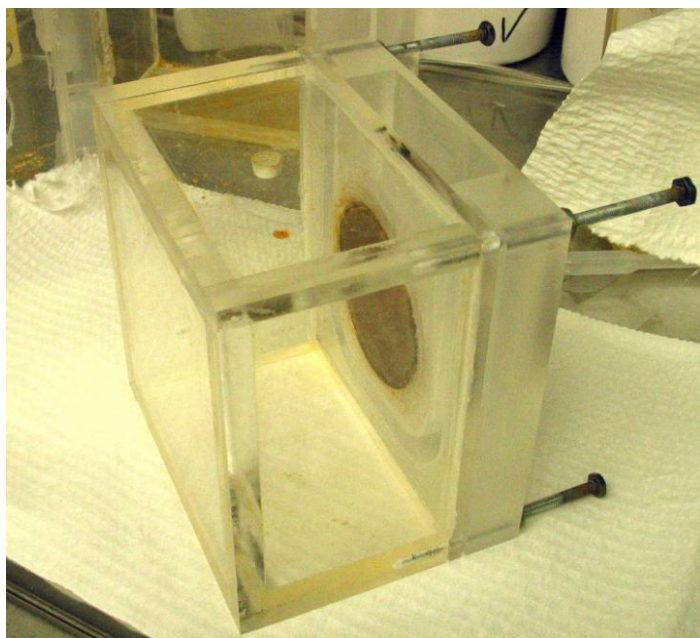


Figure 13: Diffusion Cell Loaded with Sample of Queenston Shale

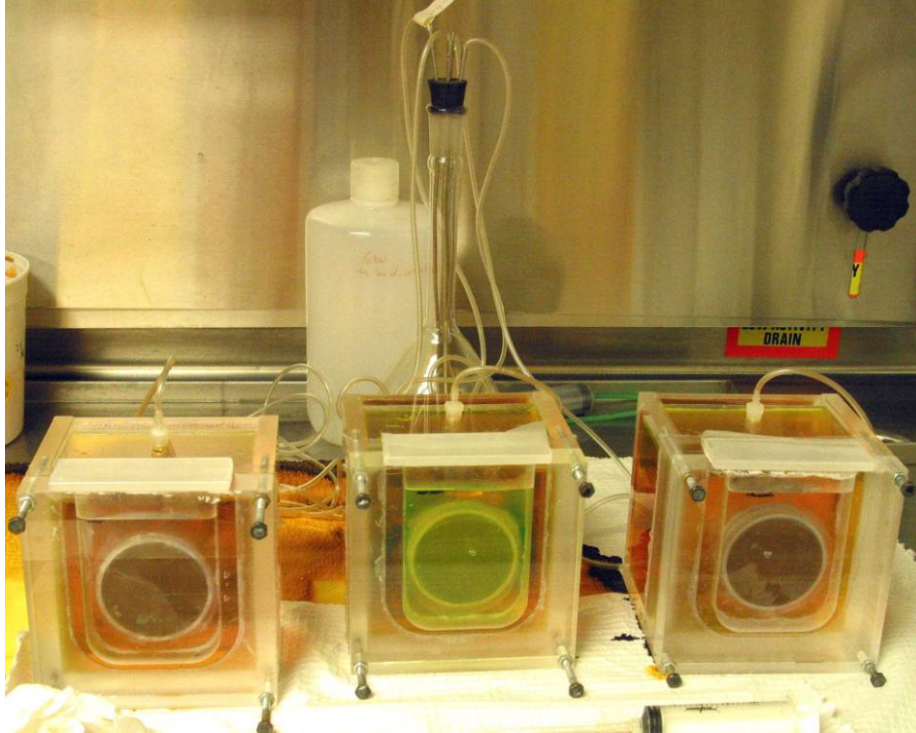


Figure 14: Three Diffusion Experiments in Progress

2.5 RADIAL DIFFUSION EXPERIMENTS

Radial diffusion experiments may be performed if core of suitable size is available. Radial diffusion experiments are conducted to test the effects of rock heterogeneity and its effect on REV. The samples used in radial diffusion experiments are larger than those in the standard diffusion cell experiments, allowing diffusion measurements over longer distances. In the radial experiments, the diffusive flux from the entire sample is used to determine an average effective diffusion coefficient that takes into account all of the sample heterogeneity. This value can be compared to effective diffusion coefficients estimated from diffusion profiles that sample specific sections of the rock sample, chosen to reflect sample variability. The diffusion profiles obtained from these controlled laboratory tests provide a useful comparison to element concentration gradients observed in nature, which have been attributed to natural diffusion processes (e.g. Gimmi and Waber 2004).

A radial diffusion experiment consists of a 150 mm long core with a 200 to 300 mm diameter. A 36 mm diameter hole is cut along the central axis of the core to serve as a tracer reservoir (Figure 15). A radial Plexiglas diffusion cell (Figure 15) is constructed to provide a several mm wide space around the outside of the core that would function as the elution reservoir. A Plexiglas plate is secured to the bottom of the core using silicon to seal the bottom of the tracer reservoir. Another Plexiglas plate is cemented to the top of the core to provide an additional barrier between the tracer and elution reservoirs. This plate has an opening in the middle to allow access to the tracer reservoir, and another opening at the edge to allow access to the elution reservoir. Once the core is placed into the diffusion cell, a lid is attached to the top of the cell to provide an airtight seal. This makes it possible to draw a vacuum inside the cell to

help saturate the rock before the diffusion experiment. While the entire contents of the diffusion cell can be isolated from the atmosphere, the tops of the tracer and elution reservoirs are left open to the same atmosphere within the diffusion cell.

Once the rock core has been placed into the diffusion cells, the core is allowed to saturate with de-aerated water under a vacuum. Diffusion experiments are initiated by removing the filling solution from the tracer reservoir and replacing it with tracer solution. The levels of the tracer and elution reservoirs are carefully checked to make sure they are at the same hydraulic head. Periodically, the elution reservoir is sampled by removing 20 mL of solution, which is immediately replaced by 20 mL of tracer-free solution.

A radial diffusion experiment is terminated by removing the tracer and eluant solutions and then cutting small diameter cores (20 mm diameter) at right angles to the core axis. These cores are cut into 5 mm long pieces, which are leached in 10 mL volumes of deionized water for 30 days to estimate tracer concentrations. After converting the measured tracer concentrations to pore water concentrations (Vilks et al. 2004), the results are used to construct diffusion profiles.

Radial diffusion experiments were not performed with sedimentary rocks in this study because large diameter (200 to 300 mm) core was not available. However, the methodology is included here for completeness, as an additional experimental method which could be applied to determine the diffusive properties of sedimentary rocks.

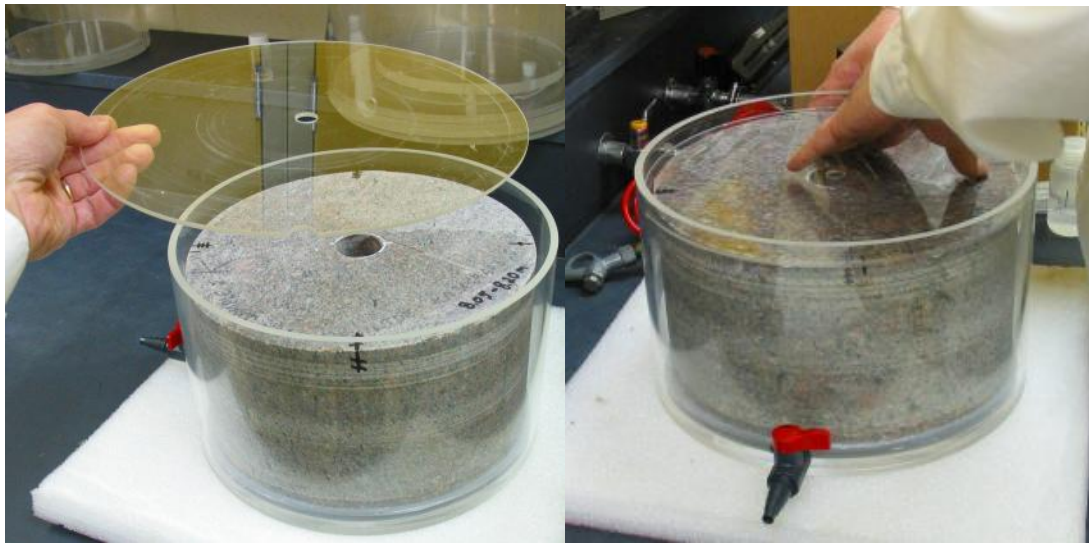


Figure 15: Installing a Radial Diffusion Experiment

2.6 PERMEABILITY ESTIMATION

Permeabilities of selected core samples are estimated at various confining pressures using the High Pressure Radioisotope Migration apparatus (HPRM), described by Drew and Vandergraaf 1989. The HPRM consists of a core holder assembly, which is placed in a pressure vessel that can be operated with a maximum pressure of about 20 MPa. Core samples, with lengths of 2.0 cm, are placed between two stainless steel cylinders (Figure 16), each containing a centre drilled hole. The core samples and stainless steel cylinders are coated with a pliable coating to isolate the circumference of the core from the water used as the pressure medium in the pressure vessel (Figure 17). Once the core and stainless steel cylinders are connected to the lines used to pass sample fluid through the core, the pressure vessel is assembled and partially filled with water. A confining pressure is applied to the pressure vessel, which subjects the core sample to a tri-axial pressure along its length and both ends. Water is then pumped through the core at a constant flow rate and the pressure differential between the inlet and outlet side of the core is measured. Provided that the inlet pressure is not allowed to exceed the confining pressure, water flow is always from one end of the core to the other end, following the interconnected pore spacings. The flow rate is determined by measuring the mass of water collected at the outlet over a given time interval. The HPRM equipment is illustrated in Figure 18.

The permeability of the core is given by

$$k = \frac{QL\mu}{A\Delta P} \quad (16)$$

where

- | | |
|----|---|
| k | is the permeability in m ² , |
| Q | is the volumetric flow rate in m ³ /s, |
| L | is the length of the core in m, |
| μ | is the viscosity of the transport solution in N·s/m ² , |
| A | is the cross sectional area of the core in m ² , and |
| ΔP | is the pressure differential between the inlet and outlet of the core in N/m ² ; |

Rock samples used for permeability estimation have a 25 mm diameter. These can be drilled from selected core samples using an orientation that is either parallel or perpendicular to the bedding planes.

In addition to sample dimensions, the parameters measured to calculate permeability consist of:

- The volumetric flow rate, Q, which is determined by collecting water for a measured time period. The volume of collected water is determined gravimetrically using a balance that is checked with weights that have their mass traceable to an ASTM Class 1 calibrated weight set.
- Pressure drop across sample, ΔP, is determined by a pressure transducer measuring the pressure of water being applied to one end of the sample. The pressure transducer is calibrated with a deadweight tester on a regular basis.

The error associated with a permeability measurement is the sum of errors from (1) the area of the sample cross section, (2) the sample length, (3) the pressure drop across the sample, and (4) the measured flow rate. The error attributed to the area of the cross section is about 1.6 percent. The error associated with sample length depends upon the total sample length, and varies between 4 and 5 percent for the samples used in this study. The error attributed to the pressure drop across the sample also depends on the magnitude of the pressure drop, typically varying between 1 and 20 percent. The error associated with the flow rate measurement is influenced by the total measured mass of fluid, as well as the time used to collect a given volume of fluid. Errors associated with flow rate measurements varied from 0.4 to 20 percent.



Figure 16: Rock Core Sample (shale) Enclosed by End Pieces to be Used in a Permeability Measurement



Figure 17: Rock Core Sample Coated with Silicon and Ready to be Loaded in Pressure Vessel for Permeability Measurement

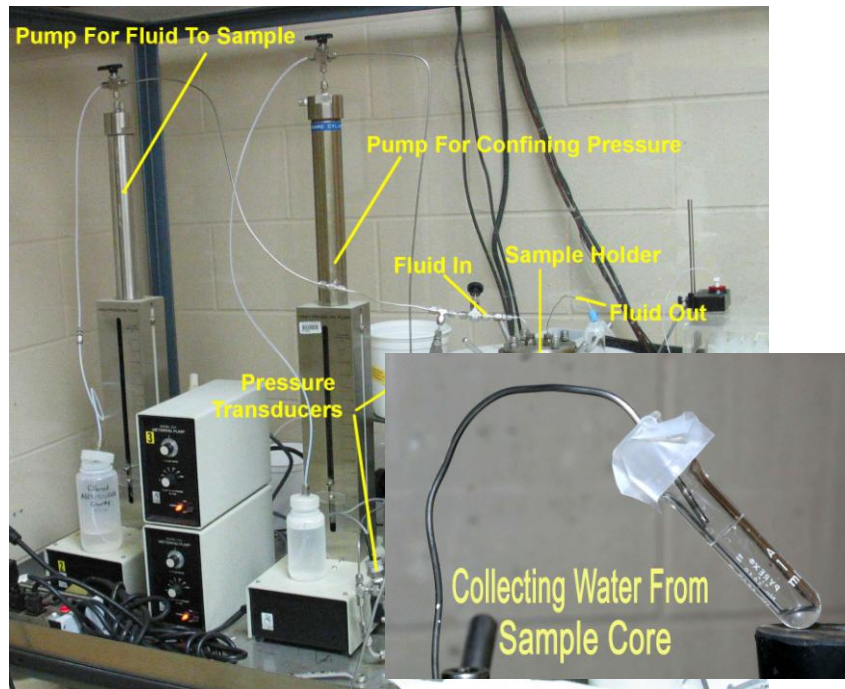


Figure 18: HPRM Facility for Measuring Permeability

2.7 ESTIMATION OF PORE FLUID COMPOSITION

An understanding of pore fluid chemistry in sedimentary rocks is important for formulating the composition of solutions used in laboratory diffusion experiments. The ionic strength of pore fluids will influence the porosity available for the diffusion of anions. In dilute waters the diffuse double layer around mineral surfaces will be relatively thick, and restrict the porosity available to the diffusion of iodide. In saline waters the double layer thickness will be significantly reduced, providing more porosity for anion diffusion (Appelo and Postma, 1994). To minimize any experimental artifacts due to differing ionic strengths between the tracer and effluent solutions and the pore water itself, the pH, the Eh and ion composition of solutions used in diffusion experiments can be designed to be as similar to the pore water composition as possible. This also minimizes water-rock interactions such as dissolution or precipitation reactions that could alter the porosity of the core sample during the course of the experiment. Therefore, to obtain diffusion parameters that are relevant to in-situ conditions, synthetic porewaters can be used to match the chemical composition of the tracer and effluent solutions to in-situ pore water compositions as closely as possible.

Pore fluid compositions can be estimated by extracting pore fluids from rock samples or by assuming that groundwater collected from rock formations provides a reasonable approximation to pore fluid chemistry. However, this latter assumption may not be well founded, given that the rock matrix may have a very low permeability compared to water conducting fractures. Profiles of chloride and stable isotopes measured in pore waters across a low-permeability stratigraphic sequence have shown that these parameters vary across different formations (Gimmi and Waber 2004), and may not be the same as the waters sampled in boreholes from higher-

permeability water-conducting features. An estimation of the in-situ pore water composition can be obtained using rock core from the formation of interest.

The extraction of pore fluids from low porosity rocks is not straightforward and may involve uncertainty associated with the understanding of rock matrix porosity and the possible sample penetration by drilling fluids. The major components of pore fluids will consist of soluble salts. A simple method of extracting these salts involves leaching small rock coupons in a known volume of deionized water for a period of about 30 days (Vilks et al. 1999).

The following method was tested with samples of Queenston shale, Whirlpool sandstone and Cobourg limestone, to estimate pore fluid compositions. These estimates can then be used to design synthetic pore waters for use in the diffusion experiments. Rock samples are first crushed into gravel-sized pieces. The intent is to facilitate the extraction of salts in connected pore spaces by increasing the sample surface area. However, the sample is not crushed to a fine powder to avoid breaking mineral grains and exposing fluid inclusions. The crushed rock is suspended in 20 to 25 mL of deionized water and stored in centrifuge tubes (Figure 19). The samples are periodically shaken to homogenize the leachate composition. The samples are allowed to leach for at least 30 days, after which they are centrifuged. The supernatant is then removed and analyzed for anions and cations. Blank solutions with deionized water and no rock sample are included to check for contamination. After the first leach, a second leach may be initiated by adding another 25 mL of deionized water and allowing the samples leach for another 30 days.



Figure 19: Shale Samples Being Leached to Determine Pore Fluid Composition

3. RESULTS

3.1 POROSITY

Porosity values estimated using the water immersion method are given in Table 2 for samples of Queenston shale. The parameters that appear in the left column are defined by Eqs. 1 to 3 in Section 2.2.2. The average shale porosity was 6.63 ± 0.48 percent.

Table 2: Porosity Values Derived from Queenston Shale

Depth (m)	84.0	84.0	93.4	101.7	101.7	104.8	104.8
W_D	14.3909	21.2236	18.1422	34.9703	29.1124	28.0417	25.6109
W_s	14.7257	21.7978	18.6365	35.8692	29.8948	28.7179	26.2070
W_{vs}	9.2717	13.6539	11.6537	22.5950	18.7964	17.8961	16.3976
V_s	5.4662	8.1621	6.9984	13.3038	11.1231	10.8460	9.8313
V_w	0.3355	0.5755	0.4954	0.9009	0.7841	0.6777	0.5974
Porosity	0.061	0.071	0.071	0.068	0.070	0.062	0.061

In contrast to Queenston shale, samples of Lindsay limestone displayed excellent stability and could be handled in the same way as samples of crystalline rock. In the interests of method development, limestone porosity was estimated by water immersion using both the original protocol used for crystalline rock (dry weight determined by vacuum drying) and the newer method modified for sedimentary rocks. Following the original protocol, samples of Cobourg limestone were dried under vacuum for over 30 days. Samples were periodically weighed to follow the drying process (Figure 20). Rapid water loss occurred within the first 6 days, followed by a period of slow drying. Although the drying curves appeared to level off after about 30 days, a prolonged drying period would probably have produced further weight loss. After the period of vacuum drying, the samples were placed in an oven to determine the oven-dried weight.

Porosity values estimated for Cobourg limestone are summarized in Table 3. Dry weights determined by oven drying were consistently lower by 0.2% than those measured by vacuum drying. Extending the vacuum drying times to several years would not significantly affect the outcome. The porosities determined by oven drying were about 30 percent higher than those estimated using vacuum drying. Assuming that oven drying produces a better estimate of dry weight, the estimated average porosity of Cobourg limestone was 1.71 ± 0.27 percent.

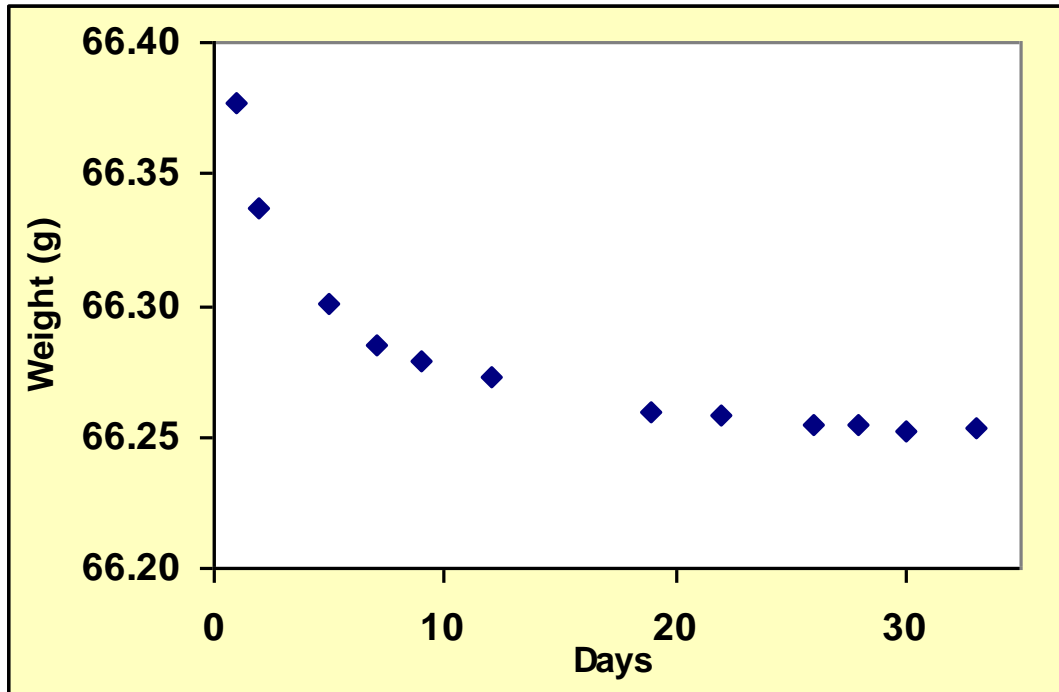


Figure 20: Example of Drying Curve (Core #4) to Determine the Dry Weight of Limestone Sample

Table 3: Porosity Values Derived for Cobourg Limestone

	Core #4	Core #9	Core #10	Rectangle
W_D (Vacuum Dry)	66.2529	56.7595	60.5911	71.4187
W_D (Oven Dry)	66.1451	56.6581	60.4513	71.2465
W_s	66.5106	56.9745	60.9055	71.7455
W_{vs}	41.8176	35.7976	38.2322	45.0774
V_s	24.7482	21.2242	22.7240	26.7277
V_w (Vacuum Dry)	0.2583	0.2155	0.3151	0.3276
V_w (Oven Dry)	0.3663	0.3171	0.4552	0.5002
Porosity (Vacuum Dry Wt)	0.0104	0.0102	0.0139	0.0123
Porosity (Oven Dry Wt)	0.0148	0.0149	0.0200	0.0187

3.2 MERCURY INTRUSION POROSIMETRY RESULTS

Typical pore size distributions determined by mercury intrusion porosimetry for Queenston shale and Cobourg limestone are illustrated in Figure 21. The plots clearly show that sandstone is dominated by large pore sizes, while shale and limestone have significantly smaller pores in the nanometer range. MIP data are summarized in Table 4 for shale, and in Table 5 for limestone. As indicated by the pore size distribution plots, the median pore diameter for shale and limestone are very small, ranging from 4.9 to 10 nm. The MIP porosity values for shale were a factor 1.6 to 2.2 lower than the porosities estimated by water immersion. The difference can likely be attributed to the inability of mercury to penetrate pore spaces smaller than 3 nm. The MIP porosity determined for Cobourg limestone is closer to that estimated by water immersion, being only a factor 1.2 to 1.7 lower. Interestingly, the MIP porosity values for limestone were in most cases higher than water immersion estimates if one were to use vacuum drying to determine the dry sample weight. This supports the conclusion that vacuum drying is not sufficient to determine a dry sample weight.

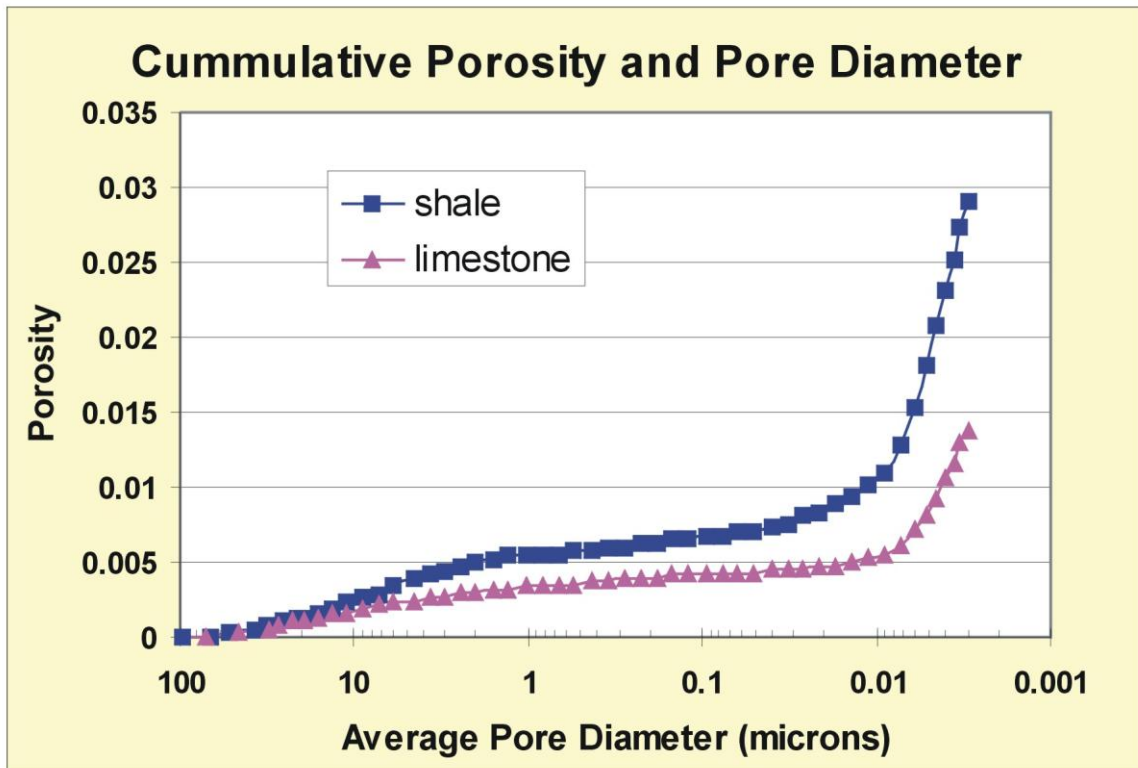


Figure 21: Typical Pore Size Distributions for Shale and Limestone

Table 4: MIP Data for Queenston Shale

Depth (m)	84.0	84.0	93.4	101.7	101.7	104.8	104.8
Rock Type	Shale						
Median Pore Diameter (nm)	5.9	6.4	6.8	4.9	5.5	6.2	7.6
Bulk Density (g/mL)	2.6537	2.6148	2.6207	2.6334	2.6231	2.2354	2.6022
Porosity (%)	3.83	4.12	4.25	3.43	3.83	2.79	3.62
% of stem used	23	25	27	21	23	18	19

Table 5: MIP Data for Cobourg Limestone

	Core #4	Core #9	Core #10	Rectangle
Median Pore Diameter (nm)	7.5	7.1	10	6.3
Bulk Density (g/mL)	2.6532	2.6431	2.6461	2.6399
Porosity (%)	1.22	1.23	1.19	1.38
% of stem used	6	8	7	9

3.3 THROUGH-DIFFUSION CELL MEASUREMENTS

3.3.1 Effect of Sample Thickness

The thickness of core samples used in diffusion experiments can be varied in order to optimize experimental times, while obtaining data that are statistically meaningful and capture the Representative Elementary Volume (REV). The REV is the minimum sample volume that captures all of the physical features of the rock that determine the rock parameter being estimated. Figure 22 illustrates iodide mass diffusion plots for sample of Queenston shale with thicknesses of 5 mm, 10 mm, and 30 mm. An experiment was performed with a sample with a 20 mm thickness, but unfortunately it was unusable for this comparison because the diffusion results indicated the presence of a fracture. The time required to reach steady-state diffusion progressively increases with increased sample thickness. While an experiment with a 5 mm sample could be completed in about 15 to 20 days, 60 to 90 days were required to reach steady-state in an experiment with a 30 mm sample. Experimental times for a weakly sorbing tracer, such as uranine, would be about a factor of 3 longer. A comparison of diffusion parameters determined with samples of Queenston shale having different thicknesses (identified as REV) is given in the bottom part of Table 7 (in Section 3.3.3). Effective diffusion coefficients determined with 10 mm samples were about 3 to 15 percent lower than those obtained with 5 mm samples. If the experiment with the 30 cm sample thickness had been given more time to reach steady-state, it would have produced similar results to the 10 mm sample. A sample thickness of 10 mm is the most common thickness reported in the literature

for use in diffusion studies of shales. Because the results suggest that an experimental thickness of 10 mm is sufficient to capture the REV, the standard sample thickness for use in diffusion experiments with shale samples was set to 10 mm.

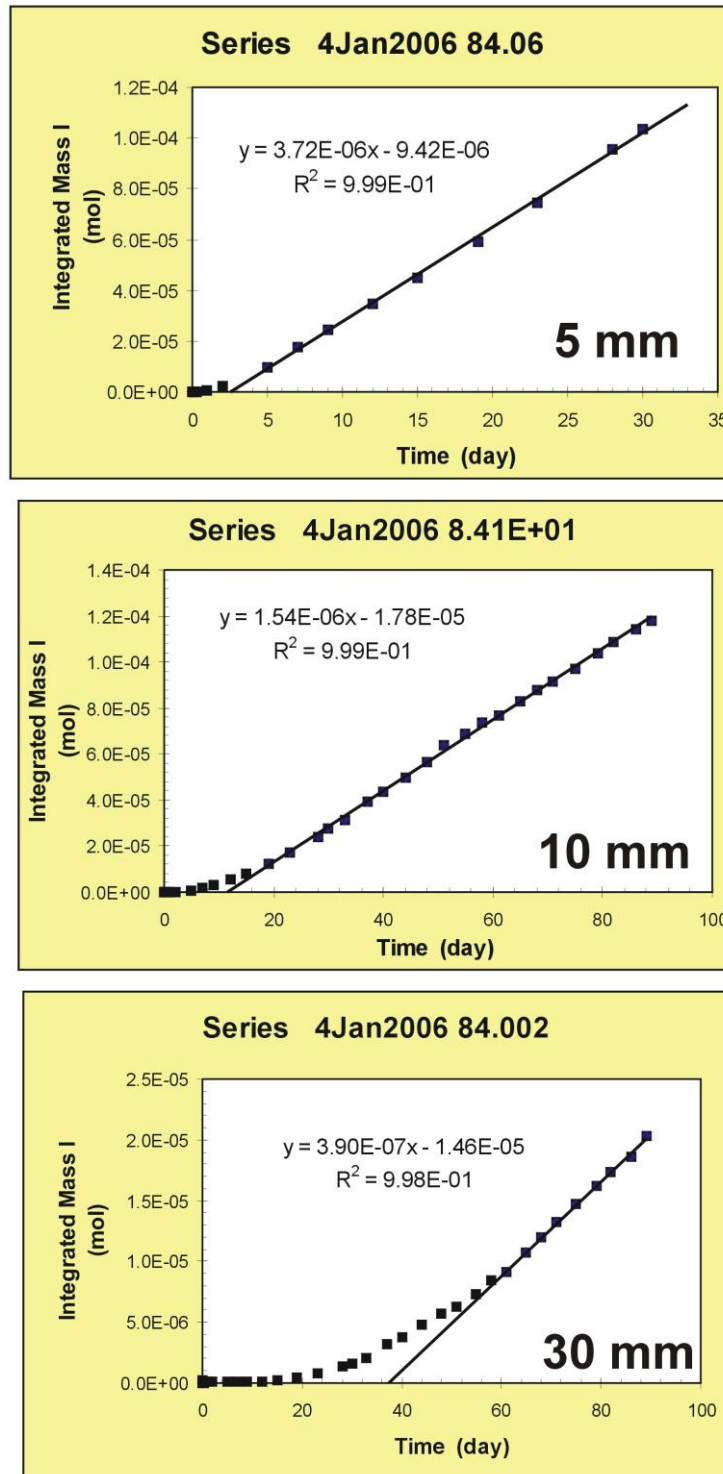


Figure 22: Iodide Mass Diffusion Plots for Samples of Queenston Shale with Thicknesses of 5, 10, and 30 mm

The effect of sample thickness on diffusion parameters estimated for limestone can be seen in the bottom part of Table 8 (in Section 3.3.3), with samples designated as REV. As for the shale samples, experimental times of 10 to 25 days were adequate for samples with a thickness of 10 mm. Significantly longer experimental times (40 to 100 days) were required for samples with thicknesses of 20 and 30 mm. Iodide and tritium diffusion coefficients were observed to decrease with increasing sample thickness. The iodide effective diffusion coefficient decreased by 15 percent as the sample thickness was increased from 6 mm to 10 mm, and decreased a further 16 percent as sample thickness was increased to 20 mm. The 20 mm and 30 mm samples produced identical iodide effective diffusion coefficients. Although the tritium effective diffusion coefficient decreased by 19 percent as sample thickness was increased to 10 mm, the effective diffusion coefficients were not significantly different in the samples with thicknesses of 10 mm to 30 mm. A standard sample thickness of 10 mm was used for estimating diffusion parameters for Cobourg limestone, to be consistent with measurements made with shale samples and because the diffusion results did not show a significant reduction in the tritium diffusion coefficients in samples thicker than 10 mm.

3.3.2 Stability of Shale Samples

During sampling of the core, the Queenston shale was found to be a stable, relatively hard material. Striking the core with a hammer caused it to break along planes that were roughly perpendicular to the core axis. However, when core slices up to several cm in thickness were immersed in water, it was found that the core began to break up within several hours, depending upon the salt content of the water. The break-up pattern (Figure 23) did not appear to follow bedding planes, and instead followed irregular features that appear similar to a blocky, quasi-nodular structure that can be seen in cores. The origins of this structure might be related to a combination of processes that could include particulate transport, local intense mudcracking and early diagenetic processes (Broglly et al., 1998). After prolonged contact (weeks) with water, the broken pieces of shale remained intact, without further disintegration. This suggests that the alteration process only occurred along the aforementioned features, with little or no penetration of the shale matrix.



Figure 23: Core Slice of Queenston Shale Immersed in 170 g/L KNO₃ Showing a Parting Pattern Typical of Unconfined Samples Immersed in Water

As mentioned previously, this sample instability has been accounted for in the revised procedure used to estimate rock porosity. Although it was anticipated that sample instability could pose a problem for diffusion experiments, shale samples mounted in sample holders (Figure 4 and Figure 13) appeared to remain stable when contacted with tracers and eluant solution. Because the shale samples in the diffusion cells were exposed to 17 g/L KNO_3 solutions, it was initially believed that the higher salinity of these solutions (compared to deionized water) may have played a role in stabilizing the shale samples. However, when unconfined samples were placed in 17 g/L and even 170 g/L (Figure 23) solutions, they still disintegrated. The only difference with deionized water was that the presence of salt slowed the disintegration rate slightly.

In most cases, any changes in the shale samples were not significant enough to produce changes in diffusion rates for time periods up to 90 days, as illustrated in Figure 22. If sample disintegration had begun some time during the diffusion test, one would expect to observe an increase in the slope of the mass flux. Although sample disintegration was not observed, changes in sample properties did occur in some cases. For example, Figure 24 shows that iodide diffusion reached a steady state after about 30 days. However, some time after 50 days, there was a change in sample properties resulting in a reduced diffusive flux. This sort of effect has been observed in altered crystalline rock and may be attributable to changes in pore geometry caused by clay swelling or other mineral alteration. In sedimentary rocks, it might be expected that sample alteration due to the dissolution or precipitation of salts may be more frequently observed in diffusion experiments. The impact of these effects could be minimized by (1) designing experiments with shorter diffusion times, (2) matching the composition of experimental solutions with actual pore fluid compositions as closely as possible, and (3) ensuring that the number of experiments that are initiated is large enough to allow for the failure of some tests.

When a shale sample is loaded into a diffusion cell, the zones of weakness observed in Figure 23 are not visible upon close inspection. However, once the diffusion experiment is initiated, the presence of a fracture or a parting plane may become evident very quickly, and observed as a rapid tracer breakthrough and resulting diffusion coefficients and rock capacity values that are significantly higher than measured for similar samples. Such experiments could be terminated and restarted with fresh samples. On the other hand, diffusion coefficients determined from samples containing fractures could be used to place an upper bound on the range of D_e values in sedimentary rocks. Figure 24 and Figure 25 illustrate an example of iodide and tritium diffusion in a “defective” sample that contained a fast flow path. Although shortly after being initiated it was suspected that this sample contained a fast transport path, the experiment was maintained to document the effects of a “defective sample”. Interestingly, after 50 days the fast transport path appears to have become obstructed and the resulting decrease in diffusion produced iodide and tritium D_e values that are similar to samples without fractures.

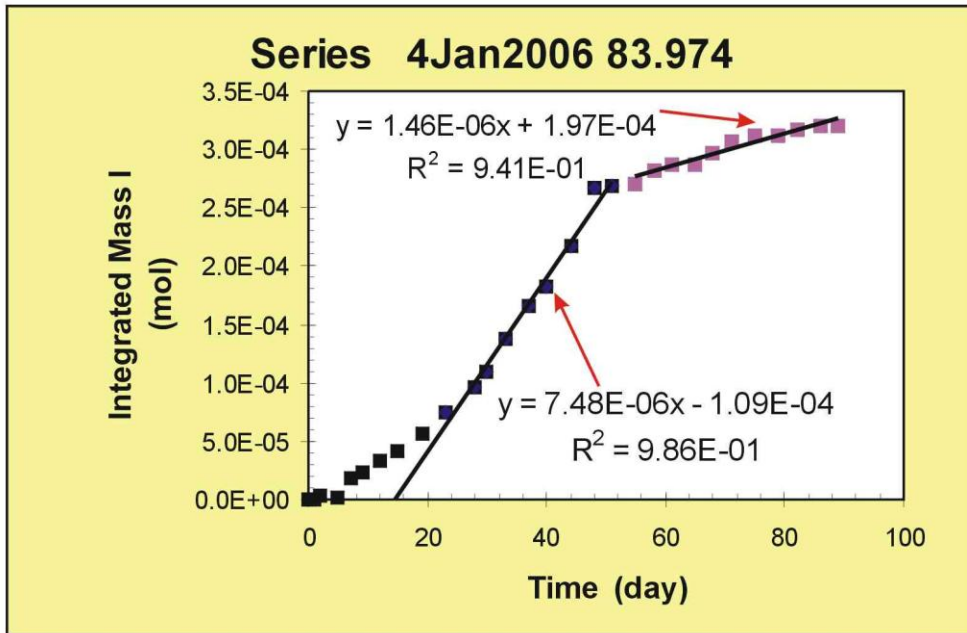


Figure 24: Iodide Diffusion in a Shale Sample (REV 20 mm) Containing a Zone of Fast Transport

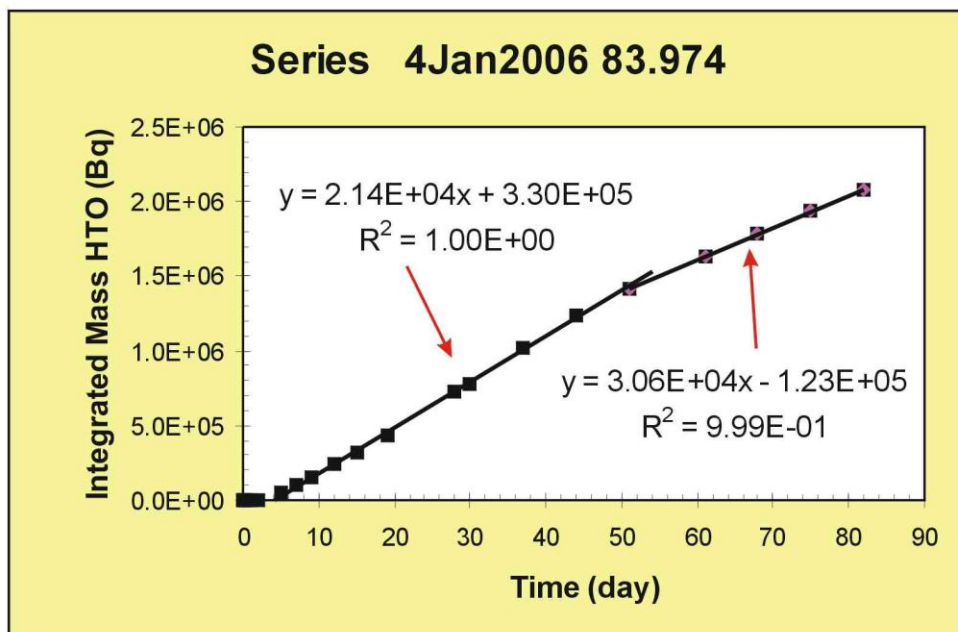


Figure 25: Tritium Diffusion in a Shale Sample (REV 20 mm) Containing a Zone of Fast Transport

3.3.3 Effective Diffusion Coefficients for Shales and Limestone

A total of 24 diffusion cell experiments were performed to characterize diffusion parameters in shales and limestones, as summarized in Table 6. With the exception of samples used to check REV, the standard sample thickness used in diffusion experiments was 10 mm (Section 3.3.1). With the Queenston shale, samples were selected from a range of depths to examine whether sample depth has any effect on estimated diffusion coefficients. Most samples were core slices and therefore were used to estimate diffusion perpendicular to bedding planes. Two shale samples were cut as slabs parallel to the core axis, with the intention of measuring diffusion parallel to bedding. This cutting operation was performed dry, without using water or any other coolant in order to prevent sample spalling as a result of rewetting. The choice of samples of Cobourg limestone followed a similar approach. Finally, two shale and two limestone samples were used to evaluate the effect of pore water composition on estimated diffusion coefficients.

Table 6: Sample Matrix for Diffusion Cell Experiments

Formation	Comment	No. of Samples
Queenston Sh.	78 m depth:	2
	84 m depth: check REV	4
	105 m depth:	2
	87 m depth: diffusion parallel to bedding	1
	96 m depth: diffusion parallel to bedding	1
	88.5 m depth: synthetic pore water	2
Cobourg Limestone	36.5 m depth:	3
	36.5 m depth: check diffusion parallel to bedding	1
	43.8 m depth:	1
	43.8 m depth: check diffusion parallel to bedding	1
	55.7 m depth: check REV	4
	55.9 m depth: synthetic pore water	2

The results of iodide and tritium diffusion experiments are summarized in Table 7 for Queenston shale and Table 8 for Cobourg limestone. Effective tortuosity values were calculated using Eq. (7) and porosity values estimated by water immersion.

In Queenston shale samples there appears to be a 30% decrease in iodide and tritium diffusion coefficients with increasing sample depth from 85 to 105m, which may suggest that greater burial depth has reduced the diffusive properties of shale. In the limestone samples, the iodide and tritium diffusion coefficients were higher by a factor 2.6 to 2.9 in samples taken from greater depths. However, the number of measurements was insufficient to conclude whether this variation can be attributed to slight changes in lithology or to the effects of burial depth.

Table 7: Iodide and Tritium Diffusion Parameters for Queenston Shale

Sample	Iodide De (m ² /s)	% I Rock Cap.	I τ _D	Tritium De (m ² /s)	% HTO Rock Cap.	HTO τ _D
RESULTS USING SOLUTIONS WITH TDS OF 17 g/L						
78 m	(1.26±0.03) X 10 ⁻¹²	4.1±0.2	12	(1.0±0.2) X 10 ⁻¹¹	13±9	9.2
78 m	(1.66±0.03) X 10 ⁻¹²	4.5±0.2	11	(1.3±0.2) X 10 ⁻¹¹	17±9	8.4
84 m	(1.04±0.01) X 10 ⁻¹²	4.9±0.2	11	(1.12±0.02) X 10 ⁻¹¹	6±2	7.6
105 m	(8.7±0.2) X 10 ⁻¹³	2.9±0.1	10	(7.3±1.2) X 10 ⁻¹²	9±6	7.8
105 m	(1.12±0.02) X 10 ⁻¹²	3.4±0.1	8.9	(8.9±1.3) X 10 ⁻¹²	9±8	7.1
87 bed	(1.6±0.2) X 10 ⁻¹²	2.43±0.01	9.2	(1.5±0.6) X 10 ⁻¹¹	8.9±0.2	6.4
96 bed	(9.4±0.5) X 10 ⁻¹³	2.44±0.05	12	(1.28±0.04) X 10 ⁻¹¹	4.6±0.7	7.0
with fracture	(9.0±0.4) X 10 ⁻¹²	19±2	3.8	(1.81±0.02) X 10 ⁻¹¹	9.3±0.8	5.9
REV 5 mm	(1.23±0.02) X 10 ⁻¹²	5.9±0.6	11	(1.25±0.02) X 10 ⁻¹¹	9±4	7.2
REV 10 mm	(1.04±0.01) X 10 ⁻¹²	4.9±0.2	11	(1.2±0.2) X 10 ⁻¹¹	9±3	7.1
REV 30 mm	(7.5±0.1) X 10 ⁻¹³	1.52±0.04	14	(9.02±0.02) X 10 ⁻¹²	6.4±0.3	8.3
RESULTS USING SOLUTIONS WITH TDS OF 290 g/L						
88.5 m	(2.44±0.06) X 10 ⁻¹²	3.6±0.6	7.4	(1.86±0.02) X 10 ⁻¹¹	9.6±0.3	5.9
88.5 m	(2.55±0.04) X 10 ⁻¹²	3.1±0.4	7.3	(1.90±0.02) X 10 ⁻¹¹	10.7±0.2	5.8

The respective average values of iodide and tritium effective diffusion coefficients for shale samples measured perpendicular to bedding were $(1.2 \pm 0.3) \times 10^{-12}$ and $(1.0 \pm 0.2) \times 10^{-11}$ m²/s. Diffusion coefficient values measured parallel to bedding in shales for iodide and tritium were $(1.3 \pm 0.5) \times 10^{-12}$ and $(1.4 \pm 0.2) \times 10^{-11}$ m²/s, respectively. These values were not significantly different from those measured perpendicular to bedding, indicating that diffusion in Queenston shales is isotropic. In the limestone, the respective average diffusion coefficients for iodide and tritium measured perpendicular to bedding were $(2.5 \pm 1.5) \times 10^{-13}$ and $(2.2 \pm 1.5) \times 10^{-12}$ m²/s, while those measured parallel to bedding were $(3.4 \pm 4.4) \times 10^{-12}$ and $(8.4 \pm 8.5) \times 10^{-11}$ m²/s for iodide and tritium respectively. It should be noted that only two samples were used for estimating diffusion parallel to bedding, and that the difference in diffusion coefficient values between these two samples was about an order of magnitude. This indicates that diffusivity parallel to bedding in Cobourg limestone could be highly variable, and on average could be over an order of magnitude higher than perpendicular to bedding. A larger number of measurements would be required to verify these initial findings.

Table 8: Iodide and Tritium Diffusion Parameters for Cobourg Limestone

Sample	Iodide De (m ² /s)	% I Rock Cap.	I τ _D	Tritium De (m ² /s)	% HTO Rock Cap.	HTO τ _D
RESULTS USING SOLUTIONS WITH TDS OF 17 g/L						
36.6 m	(2.04±0.07) X 10 ⁻¹³	1.21±0.05	12	(1.6±0.1) X 10 ⁻¹²	2.4±2.1	9.5
36.4 m	(1.60±0.02) X 10 ⁻¹³	0.53±0.02	14	(1.2±0.1) X 10 ⁻¹²	0.4±1.6	11
36.5 m	(9.5±0.3) X 10 ⁻¹⁴	0.44±0.02	21	(5.7±0.1) X 10 ⁻¹³	1.3±0.6	18
43.8 m	(4.20±0.05) X 10 ⁻¹³	1.40±0.01	9.2	(4.2±0.2) X 10 ⁻¹²	3.5±0.3	6.2
55.7 m	(3.81±0.04) X 10 ⁻¹³	1.11±0.02	9.4	(3.2±0.3) X 10 ⁻¹²	1.5±0.5	7.0
36.5 bed	(2.75±0.07) X 10 ⁻¹³	1.52±0.03	12	(2.4±0.3) X 10 ⁻¹²	2.4±1.3	8.6
43.8 bed	(7±4) X 10 ⁻¹²	9.7±0.7	2.3	(1.4±0.3) X 10 ⁻¹¹	7±3	3.4
REV 6 mm	(4.46±0.07) X 10 ⁻¹³	2.11±0.03	8.7	(4.0±0.9) X 10 ⁻¹²	2.5±1.2	6.3
REV 10 mm	(3.81±0.04) X 10 ⁻¹³	1.11±0.02	9.4	(3.2±0.3) X 10 ⁻¹²	1.5±0.5	7.0
REV 20 mm	(3.19±0.07) X 10 ⁻¹³	0.98±0.01	10	(3.1±0.2) X 10 ⁻¹²	3.4±0.1	7.2
REV 30 mm	(3.18±0.02) X 10 ⁻¹³	1.03±0.01	10	(2.7±0.1) X 10 ⁻¹²	4.9±0.3	7.6
RESULTS USING SOLUTIONS WITH TDS OF 239 g/L						
55.9 m	(1.37±0.02) X 10 ⁻¹²	3.0±0.2	5.0	(7.81±0.35) X 10 ⁻¹²	6.8±4.6	4.7
55.9 m	(6.16±0.09) X 10 ⁻¹³	1.3±0.1	7.5	(3.96±0.01) X 10 ⁻¹²	3.8±1.3	6.4

The effect of pore water chemistry on diffusion measurements can be assessed by comparing diffusion parameters determined with synthetic pore water with measurements made on 10 mm samples using 17 g/L solutions. Since the diffusion coefficients measured with synthetic pore water represent diffusion perpendicular to bedding, a comparison with measurements using the 17 g/L solutions should focus on average values of measurements made perpendicular to bedding. This distinction does not make much difference for shales, but is important for limestone. In the experiments using the synthetic pore water (bottom sections of Tables 7 and 8) the average iodide and tritium De values were a factor 1.9 higher in Queenston shale. In limestone the experiments with synthetic pore water had average iodide and tritium De values that were higher by factors of 4 and 2.7, respectively. The rock capacities determined by diffusion experiments provide a measure of the porosity used by the tracers for diffusion. The iodide and tritium rock capacities in shale were not significantly different when using synthetic pore water. However, in limestone the iodide and tritium rock capacities determined with synthetic pore water were on average a factor 2.3 higher, although the difference was almost within the error of the average values.

3.4 PERMEABILITY

Samples used for permeability estimation were selected to avoid visible fractures. Therefore, the reported values represent the permeability of the rock matrix, and are likely to be lower than values estimated from borehole intervals, which may contain water-conducting features. In addition to the previously described archived core samples, permeability measurements were also performed on a recently drilled sample of Queenston shale from the Bruce Nuclear site, near Kincardine, Ontario. This sample (DGR1-459.27) was supplied by INTERA Engineering Ltd. (Ottawa, Ontario), and was shipped wrapped in plastic to preserve the pore water content.

Results of permeability measurements at different confining pressures are provided in Table 9 and Table 10. For each measurement, the tables provide values for the pressure drop across the sample, ΔP , and the flow rate measured from the water that had passed through the sample. The parameters given in the table can be used to calculate the permeability using Eq. 16.

Table 9 and Figure 26 (A) show that estimated permeability values decrease by a factor 3 to 5 as the confining pressure is increased from 4 to 15 MPa. Depending upon burial depth and hydraulic pressures, the permeability values estimated at the higher confining pressures may be more representative of in-situ conditions. When samples are removed from depth, stress relief and possible damage during drilling may increase porosity, resulting in higher permeability values estimated with rock samples in the laboratory. The observed changes in permeability with increasing confining pressure provide a measure of rock alteration as a result of stress relief. In comparison, samples of granite from the Underground Laboratory in Manitoba (Vilks et al. 2004) showed a permeability decrease of one order of magnitude as confining pressure was increased to about 15 MPa. These granite samples had been significantly altered as a result of removal from in-situ conditions of high stress (maximum stress ranging from 30 to 60 MPa). Table 10 and Figure 26 (B) illustrate the variability in permeability values of fresh Queenston shale from the Bruce Nuclear site as a function of confining pressure. The increase in confining pressure to 15 MPa reduced the measured permeability by a factor of 26.

Average permeability values in the archived samples, taken over all confining pressures, were $(8.1 \pm 6) \times 10^{-21} \text{ m}^2$ for Queenston shale perpendicular to bedding, $(1.6 \pm 0.7) \times 10^{-21} \text{ m}^2$ for Queenston shale parallel to bedding, $(1.9 \pm 1.2) \times 10^{-22} \text{ m}^2$ for Cobourg limestone perpendicular to bedding, and $(1.1 \pm 0.7) \times 10^{-21} \text{ m}^2$ for Cobourg limestone parallel to bedding. It is interesting to note that the permeability of Queenston shale perpendicular to bedding was on average a factor 4 higher than parallel to bedding. Normally one would expect that there would be better flow parallel to bedding planes. However, the Queenston formation contains irregular parting planes that cross cut bedding and may be related to diagenetic processes (Figure 23). For example, the Queenston formation contains gypsum as thin laminae, which can either lie parallel to or cut across bedding planes (Broglie et al. 1998). These parting planes are likely to increase permeability perpendicular to bedding, particularly in core samples used in laboratory measurements. In contrast, the Cobourg limestone samples displayed a permeability perpendicular to bedding that was almost an order of magnitude lower than parallel to bedding. The permeability of Cobourg limestone is lower than that of Queenston shale, which is consistent with the lower porosity of the limestone samples, and the lack of observable fracturing. The fresh samples of Queenston shale had average permeabilities of $(5.5 \pm 6.1) \times 10^{-20} \text{ m}^2$ perpendicular to bedding and $(7.2 \pm 9.7) \times 10^{-21} \text{ m}^2$ parallel to bedding.

Table 9: Permeability Measurements of Archived Core Samples

Sample	Surface Area (cm²)	Core Length (cm)	Confining Pressure (MPa)	ΔP (MPa)	Flow Rate (m³/s)	Permeability (m²)
Queenston 101.6 m, ⊥ bedding	4.91	1.00	4.5	3.2	3.0×10^{-12}	$(2.2 \pm 0.2) \times 10^{-20}$
			4.5	3.4	1.2×10^{-12}	$(8.3 \pm 1.0) \times 10^{-21}$
			6.7	3.0	2.1×10^{-12}	$(1.6 \pm 0.1) \times 10^{-20}$
			9.1	3.2	8.7×10^{-13}	$(6.2 \pm 0.5) \times 10^{-21}$
			9.2	3.3	6.1×10^{-13}	$(4.2 \pm 0.4) \times 10^{-21}$
			10.5	4.3	9.4×10^{-13}	$(5.0 \pm 0.3) \times 10^{-21}$
			11.5	4.4	8.0×10^{-13}	$(4.2 \pm 0.3) \times 10^{-21}$
			12.1	4.7	1.1×10^{-12}	$(5.1 \pm 0.4) \times 10^{-21}$
			14.9	4.8	1.6×10^{-12}	$(7.5 \pm 0.9) \times 10^{-21}$
			14.9	5.6	7.2×10^{-13}	$(2.9 \pm 0.2) \times 10^{-21}$
Queenston 80.4 m, bedding	4.91	1.20	4.10	2.70	2.2×10^{-13}	$(2.2 \pm 0.2) \times 10^{-21}$
			4.00	2.55	2.1×10^{-13}	$(2.3 \pm 0.2) \times 10^{-21}$
			6.70	2.50	2.0×10^{-13}	$(2.2 \pm 0.2) \times 10^{-21}$
			6.80	2.40	1.6×10^{-13}	$(1.8 \pm 0.1) \times 10^{-21}$
			11.00	2.70	2.2×10^{-13}	$(2.2 \pm 0.2) \times 10^{-21}$
			11.20	3.50	2.0×10^{-13}	$(1.6 \pm 0.1) \times 10^{-21}$
			14.20	3.90	1.1×10^{-13}	$(7.6 \pm 0.9) \times 10^{-22}$
			14.20	4.80	2.5×10^{-13}	$(1.5 \pm 0.1) \times 10^{-21}$
			14.20	5.40	1.2×10^{-13}	$(6.1 \pm 0.7) \times 10^{-22}$
			14.80	6.90	1.5×10^{-13}	$(5.8 \pm 0.3) \times 10^{-22}$
Cobourg ⊥ bedding	4.91	1.50	4.70	3.60	3.7×10^{-14}	$(3.5 \pm 0.3) \times 10^{-22}$
			4.49	3.70	2.3×10^{-16}	$< 10^{-22}$
			8.10	7.00	1.5×10^{-15}	$< 10^{-22}$
			9.50	9.00	5.2×10^{-14}	$(2.0 \pm 0.2) \times 10^{-22}$
Cobourg bedding	4.91	1.50	5.10	3.40	1.8×10^{-13}	$(1.8 \pm 0.1) \times 10^{-21}$
			5.10	3.40	1.3×10^{-13}	$(1.4 \pm 0.1) \times 10^{-21}$
			5.10	3.50	1.5×10^{-13}	$(1.5 \pm 0.1) \times 10^{-21}$
			7.90	3.65	1.9×10^{-13}	$(1.8 \pm 0.2) \times 10^{-21}$
			8.50	3.70	2.3×10^{-13}	$(2.1 \pm 0.1) \times 10^{-21}$
			9.00	3.80	9.0×10^{-14}	$(8.2 \pm 1.4) \times 10^{-22}$
			8.80	3.80	2.4×10^{-13}	$(2.2 \pm 0.1) \times 10^{-21}$
			13.50	3.85	4.3×10^{-14}	$(3.8 \pm 0.8) \times 10^{-22}$
			13.50	3.85	1.3×10^{-13}	$(1.2 \pm 0.1) \times 10^{-21}$
			13.80	3.80	4.4×10^{-14}	$(4.0 \pm 0.8) \times 10^{-22}$
			12.65	3.70	1.9×10^{-13}	$(1.7 \pm 0.1) \times 10^{-21}$
			14.60	3.80	8.4×10^{-14}	$(7.6 \pm 1.0) \times 10^{-22}$
			14.80	4.20	1.5×10^{-14}	$(1.2 \pm 0.9) \times 10^{-22}$
			14.80	4.15	5.9×10^{-14}	$(4.9 \pm 0.5) \times 10^{-22}$
			15.00	9.90	2.6×10^{-13}	$(9.0 \pm 0.6) \times 10^{-22}$
			14.80	9.60	1.8×10^{-13}	$(6.4 \pm 0.3) \times 10^{-22}$

Table 10: Permeability Measurements of Fresh Queenston Shale Samples

Sample	Surface Area (cm ²)	Core Length (cm)	Confining Pressure (MPa)	ΔP (MPa)	Flow Rate (m ³ /s)	Permeability (m ²)
Queenston from Bruce Site DGR1-459.27 ⊥ bedding	4.91	0.85	6.6	3.0	2.2 x 10 ⁻¹¹	(1.5±0.1) x 10 ⁻¹⁹
			6.6	4.9	4.0 x 10 ⁻¹¹	(4.6±0.1) x 10 ⁻¹⁹
			6.6	4.8	3.0 x 10 ⁻¹¹	(1.2±0.1) x 10 ⁻¹⁹
			6.6	4.7	2.2 x 10 ⁻¹¹	(9.1±0.7) x 10 ⁻²⁰
			9.3	5.0	3.5 x 10 ⁻¹¹	(1.4±0.1) x 10 ⁻¹⁹
			9.3	5.4	6.0 x 10 ⁻¹²	(2.2±0.2) x 10 ⁻²⁰
			9.5	5.5	6.0 x 10 ⁻¹²	(2.5±0.1) x 10 ⁻²⁰
			11.9	5.5	7.1 x 10 ⁻¹²	(1.4±0.1) x 10 ⁻²⁰
			15.0	5.8	4.1 x 10 ⁻¹²	(1.3±0.2) x 10 ⁻²⁰
			15.1	5.9	3.9 x 10 ⁻¹²	(1.0±0.1) x 10 ⁻²⁰
			15.4	6.7	3.1 x 10 ⁻¹²	(9.0±0.4) x 10 ⁻²¹
			15.5	7.5	3.1 x 10 ⁻¹²	(7.8±0.4) x 10 ⁻²¹
			15.7	7.7	4.1 x 10 ⁻¹²	(1.0±0.1) x 10 ⁻²⁰
15.0	7.0	2.0 x 10 ⁻¹²	(5.6±0.3) x 10 ⁻²¹			
Queenston from Bruce Site DGR1-459.27 bedding	4.91	0.60	1.6	0.7	2.2 x 10 ⁻¹²	(4.4±0.5) x 10 ⁻²⁰
			1.7	0.4	6.6x 10 ⁻¹³	(2.3±0.4) x 10 ⁻²⁰
			2.3	1.4	4.7 x 10 ⁻¹³	(4.7±0.5) x 10 ⁻²¹
			2.7	2.3	8.1 x 10 ⁻¹³	(4.9±0.5) x 10 ⁻²¹
			5.0	2.5	1.2 x 10 ⁻¹²	(6.7±0.8) x 10 ⁻²¹
			4.9	2.6	7.6 x 10 ⁻¹³	(4.0±0.6) x 10 ⁻²¹
			5.0	2.7	1.2 x 10 ⁻¹²	(6.3±0.5) x 10 ⁻²¹
			5.3	2.7	1.4 x 10 ⁻¹²	(7.2±0.7) x 10 ⁻²¹
			9.8	2.8	1.3 x 10 ⁻¹²	(6.5±0.6) x 10 ⁻²¹
			8.1	3.4	8.4 x 10 ⁻¹³	(3.4±0.3) x 10 ⁻²¹
			10.2	3.4	1.6 x 10 ⁻¹²	(6.5±0.9) x 10 ⁻²¹
			9.8	3.6	1.2 x 10 ⁻¹²	(4.5±0.3) x 10 ⁻²¹
			13.9	3.9	9.6 x 10 ⁻¹³	(3.4±0.5) x 10 ⁻²¹
			14.5	3.9	8.3 x 10 ⁻¹³	(3.0±0.5) x 10 ⁻²¹
			14.7	3.9	1.1 x 10 ⁻¹²	(4.1±0.6) x 10 ⁻²¹
15.1	4.0	9.7 x 10 ⁻¹³	(3.4±0.3) x 10 ⁻²¹			
15.7	4.4	8.7 x 10 ⁻¹³	(2.7±0.2) x 10 ⁻²¹			
16.0	4.9	8.6 x 10 ⁻¹³	(2.4±0.3) x 10 ⁻²¹			
15.9	5.0	4.4 x 10 ⁻¹³	(1.2±0.2) x 10 ⁻²¹			
12.7	5.4	6.7 x 10 ⁻¹³	(1.7±0.1) x 10 ⁻²¹			

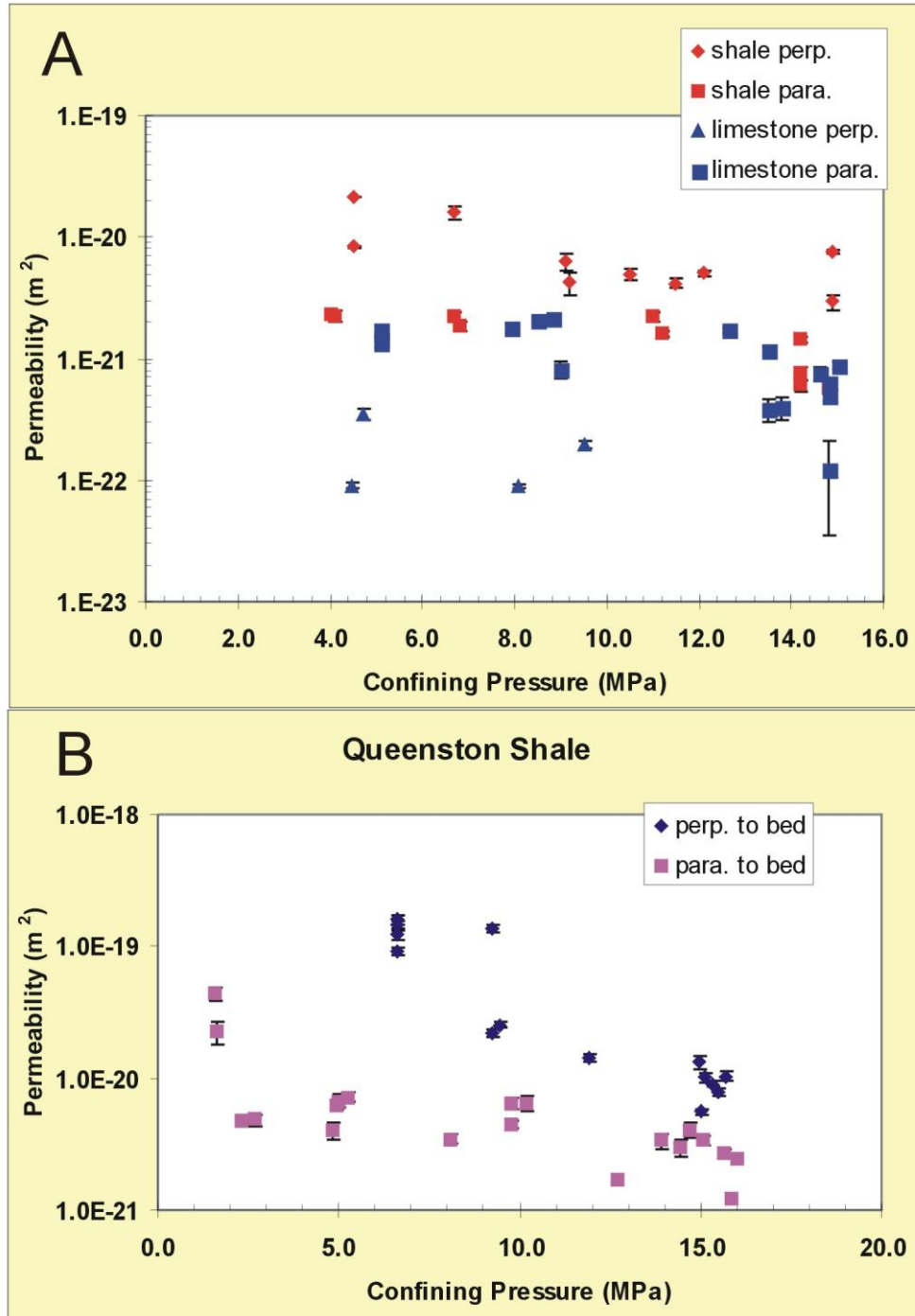


Figure 26: Effect of Confining Pressure on Permeability (Perp = perpendicular to bedding; para = parallel) for Archived Samples (A) and Shale from Bruce Site (B)

3.5 PORE FLUID COMPOSITION

The concentrations of anions and cations determined in the leachates were converted to pore water concentrations by a factor that was determined by the sample weight, the 20 to 25 mL volume of the leaching solutions, the rock density, and the estimated sample porosity. The rock density was determined from porosity measurements, which gave average values of 2.56 for sandstone, 2.66 for shale, and 2.65 for limestone. The estimated porosity for sandstone was 0.054 and the average porosities for shale and limestone were 0.060 and 0.017, respectively. Estimated pore water concentrations from the initial leaching tests are summarized in Table 11 for sandstone and shale and Table 12 for limestone. The sandstone had a TDS of 176 g/L and an ionic strength of 4.2 mol/L. The shale TDS varied from 180 to 273 g/L, corresponding to ionic strengths of 3.6 to 6.0 mol/L. Limestone had TDS values ranging from 184 to 270 g/L, corresponding to ionic strengths between 4.1 and 5.3 mol/L. The calculated charge imbalances for the Queenston shale leachates and two of the Cobourg limestone leachates were 10% or less, which is considered to be within the analytical uncertainty. The charge imbalances for the other two leachates of Cobourg limestone were greater than 10%, which may indicate either that a major species has not been analyzed, or may be indicative of analytical error in one or more of the species. Fluoride and iodide were not detected in the leachates, implying that their respective pore water concentrations were below 68 and 81 mg/L. The results in Table 11 and Table 12 are most sensitive to the porosity value used in the calculation. For example, if there is a factor 2 increase in porosity, the estimated pore water concentrations will decrease by a factor of 2. Results from the second leaching test showed negligible additional salt concentrations, except for SO₄. Relatively high SO₄ concentrations in the second leachate suggest that there is an additional source of SO₄ other than pore water salts. Dissolution of gypsum or the oxidation of sulfides are possibilities that warrant further investigation, especially for the Queenston shale, in which anhydrite/gypsum nodules were observable in hand specimen.

Table 11: Pore Water Concentrations of Anions and Cations Leached From Queenston Shale

Rock Type	Sample Depth (m)	Cl mg/L	Br mg/L	SO ₄ mg/L	Na mg/L	K mg/L	Ca mg/L	Mg mg/L	Sr mg/L	¹ Percent Charge Imbalance
Queenston SH	73.584	143441	0	519	69123	5714	15982	2357	300	2
Queenston SH	84.04	113784	648	1493	63585	5062	11713	1631	243	10
Queenston SH	84.064	130500	1560	7644	64628	5717	18643	2424	360	6
Queenston SH	90.221	122091	266	7161	62219	4578	14870	1957	325	4
Queenston SH	101.719	106554	1131	11216	57951	5515	14488	1729	290	8
Queenston SH	101.72	107646	1492	10275	58104	5749	13456	1651	275	6
Queenston SH	101.721	103844	1509	10140	55587	5742	13439	1649	275	6
Queenston SH	104.83	94533	1289	13505	49722	4911	13505	1780	264	5

¹ Negative ion balance implies an apparent excess of anions

Table 12: Pore Water Concentrations of Anions and Cations Leached From Cobourg Limestone

Rock Type	Sample Depth (m)	Cl mg/L	Br mg/L	SO ₄ mg/L	Na mg/L	K mg/L	Ca mg/L	Mg mg/L	Sr mg/L	¹ Percent Charge Imbalance
Sample 4	36.5	153540	285	25707	49077	3692	27109	9582	1239	-11
Sample 9	36.5	121610	247	22479	53949	4181	31021	11689	1439	22
Sample 10	36.5	115164	206	23267	43521	3030	23100	8704	1255	3
Rectangle	36.5	93365	92	21785	36614	2783	21053	7323	879	7

¹ Negative ion balance implies an apparent excess of anions.

4. DISCUSSION

4.1 DIFFUSIVE PROPERTIES OF SEDIMENTARY ROCKS

This study has shown that the water immersion method, using oven drying to determine dry weight, provides a good estimate of total porosity. Porosity values estimated by this method are bracketed by porosity values estimated by rock capacities determined from diffusion experiments. Porosity determined by iodide rock capacity (diffusion) was a factor 1.3 to 4 lower than that estimated by water immersion. This could be due to anion exclusion at negatively charged mineral surfaces, which reduces the total pore space available to iodide diffusion. Porosity determined by tritium rock capacity (diffusion) was similar to that estimated by water immersion. This can be attributed to the ability of hydrogen ions to diffuse into very small spaces readily accessible to water, but not necessarily to charged species such as iodide. While mercury intrusion porosimetry provides useful insight into pore sizes, it underestimated the total porosity because mercury could not be forced into pore spaces smaller than 3 nm. In summary, the water immersion method provides porosity estimates that are consistent with other methods, and it is a relatively simple method that uses commonly available laboratory equipment and can be adapted to a variety of sample shapes and sizes.

Table 13 compares values of iodide and tritium effective diffusion coefficients and water immersion porosity estimated in this study with values reported in the literature. Iodide and tritium diffusion coefficients estimated in this study for Queenston shale fell within the range of 5×10^{-13} to 1×10^{-11} (m²/s) reported for shales in Table 1. The estimated iodide and tritium diffusion coefficient values for Cobourg limestone are at the low end of values reported for limestone, from 7×10^{-13} to 1×10^{-10} (m²/s). It should be noted that the upper range of diffusion coefficient values for Cobourg limestone was determined using only one sample in which diffusion was measured parallel to bedding. Compared to other limestone formations as reported in Table 1, the tested samples of Cobourg limestone had very low diffusivity. The porosity of Queenston shale fell within the lower range of porosities reported for shales (from 1.5 to 20 percent). The porosity of Cobourg limestone was just below the porosity range (from 3 to 43 percent) reported for limestone, which is consistent with its low measured diffusivity.

Table 13: Compare Diffusion Coefficients and Porosities to Literature Values

	This Study		Literature	
	Shales	Limestone	Shales	Limestone
Iodide De (m ² /s)	8.7 x 10 ⁻¹³ to 1.7 x 10 ⁻¹²	9.5 x 10 ⁻¹⁴ to 6.6 x 10 ⁻¹²	5 x 10 ⁻¹³ to 5 x 10 ⁻¹²	7 x 10 ⁻¹³ to 3 x 10 ⁻¹⁰
Tritium De (m ² /s)	7.3 x 10 ⁻¹² to 1.5 x 10 ⁻¹¹	5.7 x 10 ⁻¹³ to 1.4 x 10 ⁻¹¹	2 x 10 ⁻¹² to 1 x 10 ⁻¹¹	3 x 10 ⁻¹² to 1 x 10 ⁻¹⁰
Porosity (%)	6.1 to 7.1	1.5 to 2.0	1.5 to 20	3 to 43

Average values of porosity, effective diffusion coefficients and permeability are presented in Table 14 to facilitate comparison of the mass transport properties of Queenston shale and Cobourg limestone. It should be noted that the results from one sample of Cobourg limestone (43.8 m and parallel to bedding) are significantly different from the other samples, and produce high standard deviations for average diffusion parameter values calculated for Cobourg limestone. The permeability results from the shale samples taken from the Bruce Nuclear site were not included in this table.

Mercury intrusion porosimetry indicated that the shale and limestone have similar average pore sizes, although the shale has a slightly smaller pore space. Taken by itself this may suggest similar diffusion properties. The average iodide effective diffusion coefficients for shale and limestone were similar, although if the high diffusivity limestone sample parallel to bedding is excluded the average iodide diffusion coefficient in limestone would be a factor 4.6 lower. The average tritium diffusion coefficient was a factor 2.8 lower in limestone, although this would increase to a factor 5.0 if the high diffusivity sample was excluded. The limestone had values of water immersion porosity, iodide rock capacity and tritium rock capacity that were smaller by factors of 3.9, 3.5 and 3.8, respectively, than those measured for Queenston shale. This indicates that to a large degree, the difference in diffusion properties can be explained by the differences in the porosities of Queenston shale and Cobourg limestone. (Note that this latter comparison excluded consideration of the high diffusivity sample, because water immersion data was not available for this sample.)

Effective diffusion coefficients for tritium were about an order of magnitude higher than values for iodide. This is explained by the tritium free water diffusion coefficient being a factor 5 higher than the iodide free water diffusion coefficient, and by the ability of tritium to use a larger portion of the pore space for diffusive mass transport.

Pore geometry also plays a role in determining effective diffusion coefficients. The parameters commonly used to approximate the effects of pore geometry are constrictivity and geometric tortuosity (Eq. 7). These terms can be combined into a single term, referred to as the effective tortuosity (Eq. 12). The calculated iodide and tritium effective tortuosities of the limestone were larger than those of shale. Although the shale had a smaller average pore size, its porosity was less tortuous and constrictive to diffusion. The effective tortuosities of tritium were smaller than those of iodide, indicating that in both rock types, the porosity used by tritium was less tortuous and less constricted than that of iodide.

The permeability of limestone was a factor 4.8 less than that of shale. This is also consistent with the limestone's lower porosity and higher effective tortuosity. Although diffusivity and

permeability are affected by porosity and pore geometry to a similar degree, the effects are not exactly the same. This is not entirely surprising because the physical processes that control resistance to chemical diffusion are different than those that determine resistance to water flowing under a hydraulic gradient.

Table 14: Average Parameter Values Affecting Mass Transport

	Queenston Shale	Cobourg Limestone
MIC Porosity (%)	3.7 ± 0.5	1.26 ± 0.09
MIC Derived Pore Size (nm)	6.2 ± 0.9	7.7 ± 1.6
Water Immersion Porosity (%)	6.63 ± 0.48	1.71 ± 0.27
Iodide Rock Capacity (%)	3.4 ± 1.1	2.3 ± 3.3
Tritium Rock Capacity (%)	9.6 ± 4.3	2.7 ± 2.3
Iodide Effective Tortuosity	10.7 ± 1.3	11. ± 5.6
Tritium Effective Tortuosity	7.6 ± 0.9	9.1 ± 4.6
Iodide De (m ² /s)	(1.2 ± 0.3) × 10 ⁻¹²	(1.2 ± 3.9) × 10 ⁻¹²
Tritium De (m ² /s)	(1.1 ± 0.3) × 10 ⁻¹¹	(3.9 ± 4.8) × 10 ⁻¹²
Permeability (m ²)	(4.5 ± 5) × 10 ⁻²¹	(9.4 ± 7.0) × 10 ⁻²²

Reported errors are standard deviations

In Table 14 the errors reported for average parameter values are standard deviations, which provide a sense of variability. A comparison of these standard deviations shows that, with the exception of tritium rock capacity, diffusion parameters have greater variability in limestone compared to shale. This suggests that further research should emphasize additional quantification of the variability in the diffusive properties of the limestone formations.

In the Queenston shale samples, there appears to be a factor 1.3 to 1.5 decrease in iodide and tritium diffusion coefficients with sample depth, suggesting that greater burial depth has reduced the diffusive properties of shale. In the limestone, the iodide and tritium diffusion coefficients were higher by a factor 2.7 to 3.3 in samples taken from the two greater depths. This could result from heterogeneities within the limestone as due to differences in lithology, or as a result of greater sample alteration in rocks removed from greater depths. The alteration would take the form of micro cracks caused by stress relief. The number of measurements is insufficient to establish the actual reason for this variation.

In shale, the iodide and tritium effective diffusion coefficients measured perpendicular to bedding were identical (within sample variability) with values measured parallel to bedding, indicating that diffusion in Queenston shales is isotropic. However, permeability measured perpendicular to bedding was a factor 4 higher than measured parallel to bedding. The permeability perpendicular to bedding was probably higher because the Queenston formation contains irregular parting planes that cross cut bedding and may be related to diagenetic processes. These parting planes may explain the increase in permeability measured perpendicular to bedding. However, these parting planes apparently did not have an effect on the diffusivity because diffusion coefficients measured parallel and perpendicular to bedding planes were identical within experimental error.

In Cobourg limestone, the average iodide and tritium effective diffusion coefficients were approximately an order of magnitude higher when measured parallel to bedding, compared to perpendicular to bedding, mainly because of high diffusivity in one sample. Only two samples were used for estimating diffusion parallel to bedding, and the difference in the diffusion coefficient values between these two samples was approximately one order of magnitude. This indicates that diffusivity parallel to bedding in Cobourg limestone is highly variable. Although permeability in Cobourg limestone is low parallel to bedding, $(1.1 \pm 0.7) \times 10^{-21} \text{ m}^2$, the permeability perpendicular to bedding appears to be an order of magnitude lower, $(1.9 \pm 1.2) \times 10^{-22}$. Therefore, in the Cobourg limestone, sample orientation appears to have the same effect on both diffusivity and permeability. However, more data points are required to establish a statistically significant database to support any conclusions regarding the effect of sample orientation on diffusivity and permeability.

The archived core samples used in this study were not drilled for the specific purpose of characterizing mass transport properties or pore water composition. No precautions were taken to prevent evaporation; the rock samples had been stored in a dried condition without any attempt to control temperature. Sample drying had the greatest impact on Queenston shale, which is known to spall when rewetted. However, adjusting experimental procedures to ensure that samples are properly constrained before being wetted was found to minimize the impact of spalling. Proper preservation of the moisture content of samples of this shale immediately after drilling may reduce or eliminate this tendency. The permeability measured with fresh Queenston shale samples also showed a significantly lower value parallel to bedding compared to perpendicular to bedding. However, on average the permeability estimated with these samples was a factor 6 higher than determined with archived samples. Given the difference in geographic location, possible rock variability, and the sample thickness of the new core was less than that of archived core, the significance of this difference has not been established.

Drying did not appear to have an effect on the integrity of Cobourg limestone samples. Drying experiments with resaturated limestone samples indicated that a significant fraction of the pore fluids would evaporate within 10 to 20 days of air-drying. A similar experiment was not performed with Queenston shale because unconfined coupons, which had been re-saturated with water, tended to break apart when exposed to air. When pore fluids evaporate, volatile elements and stable isotopes are lost. However, soluble salts are left behind. In the current study, leaching experiments were used to extract, and quantify these salts, and used to estimate pore fluid major element concentrations using measured rock porosities.

The results of leaching experiments indicated that Lower Silurian and Upper Ordovician sediments of southern Ontario have saline pore waters with TDS values ranging from 176 to 270 g/L, and corresponding ionic strengths between 3.6 and 6.0 mol/L. The average pore water element concentrations estimated for Lower Silurian Whirlpool sandstone and Upper Ordovician Queenston shale and Cobourg limestone using the leach experiments are compared to groundwater compositions from the Trenton Group (Upper Ordovician shales) and the Blue Mountain Formation (Middle to Upper Ordovician limestones) reported by McNutt et al. (1987), which are given in Table 15. As a first approximation, the high salinity pore fluids appear to be similar to the high salinity groundwaters sampled from hydrocarbon reservoirs in comparable stratigraphic horizons.

Comparing the Queenston shale pore fluids with groundwater from the Blue Mountain formation, the chloride and bromide concentrations are similar. The estimated pore fluid composition has higher sodium and potassium concentrations, and slightly higher strontium.

However, calcium and magnesium are lower in the pore fluid. The measured sulfate concentration was significantly higher in the pore fluid, possibly due to the dissolution of gypsum or the oxidation of sulfides during the leaching process. Anhydrite/gypsum nodules are visible in hand specimens of Queenston shale.

The Cobourg limestone (Michigan basin) pore fluid has similar concentrations of sodium and chloride to groundwater from the Trenton Group (Appalachian basin). The pore fluid had slightly higher concentrations of potassium, magnesium and strontium, and slightly lower calcium. Bromide was significantly lower in the pore fluid. Sulfate was again very high in the pore fluid. Because calcium concentrations are not high enough to balance the measured sulfate concentrations, another possible source for sulfate is the oxidation of sulfide. The leach experiments were conducted under atmospheric conditions, which may have resulted in the oxidation of sulfide minerals to sulfate.

In summary, the estimated pore water solutions from the leach experiments conducted as part of this study suggest the presence of high salinity water in the rock matrix. These estimated pore fluid compositions are similar to groundwater compositions sampled from oil and gas wells from formations of the same age, but different geographic locations.

Table 15: Compare Pore Water Compositions with Groundwater Compositions

	Cl g/L	Br g/L	SO ₄ g/L	Na g/L	K g/L	Ca g/L	Mg g/L	Sr g/L
<u>Pore Water - This Study</u>								
mean sandstone	69	0.49	52	22	0.7	29	2.5	0.37
mean shale	115	0.99	7.74	60	5.4	15	1.9	0.29
mean limestone	121	0.21	23.3	46	3.4	26	9.3	1.20
Ground Water – McNutt et al. (1987)								
Blue Mountain (sh)	118	1.08	0.12	22	0.4	39	4.5	0.70
Trenton Group (lim)	150	1.19	0.34	50	2.1	33	6.0	0.62

The diffusion experiments using synthetic pore water solutions suggest that the diffusion coefficients determined using the standard 17 g/L solutions could be a factor 2 to 4 lower than if measurements were performed using real pore water chemistry. In shale the total porosities used by iodide and tritium were not affected by changing pore water chemistry, suggesting that the shale porosity was not altered by the 17 g/L solutions during the experimental time frame. Also the higher ionic strength of the synthetic pore waters did not change any anion exclusion effects that could have affected iodide diffusion. In limestone the iodide and tritium rock capacities appear to be slightly higher when synthetic pore waters are used (although the differences were close to experimental variation). Since the tritium rock capacity is not influenced by anion exclusion and therefore, is not expected to be affected by salinity, the apparent increase in tritium rock capacity could be attributed to an increase in porosity.

In shale the iodide and tritium *D_e* values were a factor 1.9 higher in synthetic pore water, despite the observation that the porosity used by diffusion had not changed. Ruling out a change in porosity, one could consider several explanations for higher diffusion coefficients determined using synthetic pore waters that include (1) a higher iodide concentration in the synthetic pore waters, (2) a change in pore geometry, and (3) an experimental artefact due to

differences in the tracer and eluant solutions. The higher iodide concentration in the tracer should not be a factor because the tritium concentration was the same in both sets of experiments. A change in pore geometry also does not seem likely given that there were no apparent changes in total porosity used by diffusion. Although the ionic strengths of the tracer and eluant solutions were similar, the TDS of the tracer solution was a factor 1.7 higher. Perhaps the difference in the TDS values could have affected D_e values in shale.

In limestone the iodide and tritium D_e values determined with synthetic pore water were a factor 4 and 2.7 higher, respectively. The higher diffusion porosities could account for a portion of the differences in D_e values. If there was a change in diffusion porosity it is also conceivable that there was a change in pore geometry, resulting in a reduced effective tortuosity. The difference in the TDS values of tracer solution and eluant could also have played a role, as proposed for shale.

This study has focused on improving the understanding of mass transport processes on the scale of 1 to 3 cm. Samples were selected to be free of fractures at the macroscopic scale. Therefore, the results of this study represent a preliminary database which can be applied to improve our understanding of mass transport in the unfractured rock matrix of these two formations. One example where a fracture or a bedding plane had created a preferential transport pathway is the sample of Cobourg limestone that was cut to measure diffusion parallel to bedding (Table 8). In this sample the effective diffusion coefficients were about an order of magnitude higher than in all of the other Cobourg limestone samples, and the porosities available for diffusion had increased by factors of 7 and 2 for iodide and tritium, respectively.

Although the number of samples examined in this study was limited, the results from different sample depths suggested that in the Queenston shale, alteration by stress release during drilling did not change the diffusion parameters by more than a factor of about 3. However, it is not clear whether the same could be said regarding the sample of Cobourg limestone cut to measure diffusion parallel to bedding. Under a litho static load, would the fracture or parting responsible for the high diffusivity have been open to the same degree as in the distressed rock sample? When the confining pressure on samples of shale and limestone was increased to about 15 MPa, the permeability was reduced by a factor 3 to 5. A comparison of laboratory and in-situ measurements with granite samples removed from high stress environments showed that laboratory estimated diffusion coefficients were a factor 1 to 15 higher than in-situ values, while laboratory derived permeabilities were a factor 2 to 100 higher than in-situ values (Vilks et al. 2004). This implies that any effects of sample alteration during drilling have a more significant effect on laboratory derived permeability values, compared to effective diffusion coefficients. Furthermore, the very low laboratory derived permeability values in this study suggest that the samples were not subjected to significant alteration and therefore the derived diffusion coefficients may provide a good first approximation of matrix diffusion under in-situ conditions. This conclusion could be tested by measuring diffusion and permeability on fresh core samples taken from a broad range of depths.

4.2 SUGGESTIONS FOR FUTURE WORK

Twenty diffusion cell experiments were performed in this study to develop protocols for measuring the diffusive properties of sedimentary rocks, and to initiate a database of diffusion parameters for Ordovician sedimentary rocks of southern Ontario. Additional diffusion measurements should be performed on other Ordovician shale and limestone samples to

increase the number of measurements in the database to a statistically significant number. The enhanced database could be used to improve the understanding of the effects of burial depth, orientation with respect to bedding planes, sample alteration, and heterogeneity produced by changes in lithology with geography and with stratigraphic depth.

The results presented in this report were obtained from archived samples, which had been subjected to drying. Fresh samples, which had been sealed at the time of drilling to prevent evaporation, might provide more representative results for diffusion parameters and pore water compositions.

To resolve the question of experimental artefacts caused by pore water chemistry, it would be useful to perform a series of diffusion experiments using a range of synthetic or real pore waters. Tritium would be used as the tracer because it does not impact the ionic strength and TDS. That way the tracer and eluant solutions could have the same basic chemistry, ruling out density or osmotic effects.

The understanding of mass transport would benefit from a program of comparative laboratory and in-situ experiments. The in-situ experiments would account for the effects of natural pore water chemistry, natural stress conditions, and would not be affected by sample alteration during drilling. A comparison of in-situ results with comparative experiments could be used to validate laboratory measurements used with sedimentary rocks. In-situ experiments could also be used to evaluate the effects of sample scale on mass transport driven by diffusion or by a hydraulic gradient.

This study has focused mainly on non-sorbing tracers because of practical time constraints, and due to the fact that significantly longer experimental times that would be required to study the diffusion of sorbing tracers. At present, the understanding of contaminant sorption on shales and limestones in very saline water is limited. In addition to having knowledge of sorption reactions and sorption coefficients, the ability to use sorption to predict retardation during mass transport in a rock matrix requires an understanding of sorption/desorption kinetics and of the specific surface area available to sorption. This understanding can be obtained from mass transport experiments that use either diffusion or a hydraulic gradient. The HPRM may be of particular interest to study mass transport of sorbing tracers at different confining pressures. By modifying the confining pressure, one might be able to vary the porosity available for transport and perhaps the specific surface area available to sorption.

5. CONCLUSIONS

Experimental protocols to measure the diffusive properties of sedimentary rocks have been developed in this study. An experimental program was undertaken with archived core samples of Ordovician shale and limestone to test these protocols (water immersion porosity, mercury intrusion porosimetry, diffusion cell experiments, porosity, and pore water chemistry) for characterizing the diffusive and mass transport properties of rock matrix. The results showed that Queenston shale had an average porosity of 0.0663 ± 0.0048 , and average iodide and tritium diffusion coefficients of $(1.2 \pm 0.3) \times 10^{-12}$ and $(1.1 \pm 0.2) \times 10^{-11}$ (m^2/s). These numbers are consistent with values reported for shales in the literature. The Cobourg limestone had an average porosity of 0.0171 ± 0.0027 , and average iodide and tritium diffusion coefficients of

$(1.2 \pm 3.9) \times 10^{-12}$ and $(3.9 \pm 4.8) \times 10^{-12}$ (m^2/s), respectively. These values are low compared to typical values reported for limestone in the literature. The matrix permeability of these samples was also very low, with average values of $(4.5 \pm 5) \times 10^{-21}$ (m^2) for Queenston shale and $(9.4 \pm 7.0) \times 10^{-22}$ (m^2) for Cobourg limestone.

Porosity and pore geometry determine diffusivity and permeability. Although average pore sizes are similar in Queenston shale (6.6 ± 0.5 nm) and Cobourg limestone (7.7 ± 1.6 nm), the differences in total porosity and pore geometry (as characterized by effective tortuosity) produced significant differences in diffusivity, particularly for tritium. The rock features, such as parting planes related to diagenetic processes (Queenston shale) and bedding planes (Cobourg limestone) may affect permeability and in some cases diffusion.

The present study did not show evidence of significant sample alteration as a result of stress relief during drilling, which may suggest that the reported diffusion coefficients and permeability values can be used to provide a reasonable approximation of mass transport under in-situ conditions. However, a detailed study of the diffusive properties over a greater range of depths for the sedimentary formations from southern Ontario would be required to verify this finding.

Leaching experiments to extract soluble salts indicated that the pore waters in Ordovician sediments are highly saline, with TDS values ranging from 180 to 270 g/L. As a first approximation, the high salinity pore fluids appear similar to the high salinity groundwaters sampled from producing hydrocarbon wells in comparable stratigraphic horizons.

ACKNOWLEDGEMENTS

The work described in this report was carried out by AECL with funding from NWMO Technical Program, under Contract GS02. The authors would like to gratefully acknowledge the contributions of the following individuals to the Diffusion Project. Monique Hobbs made available the archived samples of Queenston shale and Lindsay limestone. In addition, she provided useful guidance throughout the project, and contributed useful comments in the review of the final document. Peter Hayward provided training on the procedure for estimating pore structure and porosity by mercury porosimetry. Bonnie St. Denis provided formatting and proofing for the final report.

REFERENCES

- API (American Petroleum Institute). 1960. Recommended practices for core-analysis procedure, API Recommended Practice 40 (RP40); First Edition, American Petroleum Institute, Washington, DC, p 55.
- Appelo, C.A.J. and D. Postma. 1994. Geochemistry, groundwater and pollution. Rotterdam, A.A.Balkema.
- Barone, F.S., R.K. Rowe and R.M. Quigley. 1990. Laboratory determination of chloride diffusion coefficient in an intact shale. *Can. Geotech.* 27, 177-184.
- Boving, T.B. and P. Grathwohl. 2001. Tracer diffusion coefficients in sedimentary rocks: Correlation to porosity and hydraulic conductivity. *Contaminant Hydrology* 53, 85-100.
- Bradbury, M.H. and A. Green. 1985. Measurement of important parameters determining aqueous phase diffusion rates through crystalline rock matrices. *Hydrology* 82, 39-55.
- Bradbury, M.J., D. Lever and D. Kinsey. 1982. Aqueous phase diffusion in crystalline rock. *Materials Research Society Symposium Proceedings 11, (Scientific Basis for Nuclear Waste Management V)*, 569-578.
- Brogly, P.J., I.P. Martini, and G.V. Middleton. 1998. The Queenston Formation: Shale-dominated, mixed terrigenous-carbonate deposits of Upper Ordovician, semiarid, muddy shores in Ontario, Canada. *Can. J. Earth Sci.* 35, 702-719.
- Choi, J.W. and D.W. Oscarson. 1996. Diffusive transport through compacted Na- and Ca-bentonite. *Contaminant Hydrology* 22, 189-202.
- Choi, J. W., D.W. Oscarson and P.S. Hahn. 1993. The measurement of apparent diffusion coefficients in compacted clays: An assessment of methods. *Applied Clay Science* 8, 283-294.
- Cramer J.J., T.W. Melnyk and H.G. Miller. 1997. In-situ diffusion in granite: Results from scoping experiments. Atomic Energy of Canada Limited Report, AECL-11756, COG-96-656-I.
- Descostes, M., V. Blin, B. Grenut, P. Meier and E. Tevissen. 2004. HTO diffusion in Oxfordian limestone and Callovo-Oxfordian argillite formations. *Mat. Res. Soc. Symp. Proc.*, 824.
- Dorsch, J. 1997. Effective porosity and density of carbonate rocks (Maynardville Limestone and Copper Ridge Dolomite) within Bear Creek Valley on the Oak Ridge Reservation based on modern petrophysical techniques. (ORNL/GWP)-026.
- Drew, D.J. and T.T. Vandergraaf. 1989. Construction and operation of a high-pressure radioisotope migration apparatus. Atomic Energy of Canada Limited Technical Record, TR-476.

- Eriksen, T.E. and M. Jansson. 1996. Diffusion of I-, Cs+, and Sr²⁺ in compacted bentonite – anion exclusion and surface diffusion. SKB Technical Report TR-96-16.
- Fam, M.A. and M.B. Dusseault. 1998. High-frequency complex permittivity of shales (0.02-1.30 GHz). Canadian Geotechnical Journal 35, 524-531.
- Franklin, J.A. and M.B. Dusseault. 1989. Rock Engineering. USA. McGraw-Hill.
- Gimmi, T. and H.N. Waber. 2004. Modelling of profiles of stable water isotopes, chloride and chloride isotopes of pore water in argillaceous rocks in the Benken borehole. Nagra Technical Report, NTB 04-05, Nagra, Wetingen, Switzerland.
- Harvey, K.B. 1996. Measurement of diffusive properties of intact rock. Atomic Energy of Canada Limited Report, AECL-11439, COG-95-456.
- Hawlder, B.C., K.Y. Lo and I.D. Moore. 2005. Analysis of tunnel in shaly rock consisting of three-dimensional stress effects on swelling. Can. Geotech. 42, 1-12.
- Katsube, T.J., T.W. Melnyk and J.P. Hum . 1986. Pore structure from diffusion in granitic rocks. Atomic Energy of Canada Limited Technical Record, TR-381.
- Katsube, T.J., N. Scromeda and M. Williamson. 1992. Effective porosity of tight shales from the venture gas field, offshore Nova Scotia. In Current Research, Part D; Geological Survey of Canada, Paper 92-ID, 111-119.
- Martin, C.D. and B. Stimpson. 1994. The effect of sample disturbance on laboratory properties of Lac du Bonnet granite. Can. Geotech. 31, 692-702.
- Mazurek, M. 2004. Long term used nuclear fuel waste management – Geoscientific review of the sedimentary sequence in Southern Ontario. Nuclear Waste Management Organization Background Papers, 6. Technical Methods.
- Mazurek, M. F., J. Pearson, G. Volckaert and H. Bock. 2003. Features, events, and processes evaluation catalog for argillaceous media. Nuclear Energy Agency, Organization for Economic Co-operation and Development Report No. NEA4437, ISBN 92-64-02148-5.
- Melnyk, T.W. and A.M.M. Skeet. 1986. An improved technique for the determination of rock porosity. Earth Sci. 23, 1068-1074.
- Melnyk, T.W. and A.M.M. Skeet. 1987. A mathematical study of the influence of pore geometry on diffusion. Atomic Energy of Canada Limited Report, AECL-9075.
- Ohlsson, Y. and I. Neretnieks. 1995. Literature survey of matrix diffusion theory and of experiments and data including natural analogues. SKB Technical Report, 95-12.
- Olin, M., M Valkiainen and H. Aalto. 1997. Matrix diffusion in crystalline rocks: Coupling of anion exclusion, surface diffusion, and surface complexation. VTT Chemical Technology Report, POSIVA-96-25.

- Oscarson, D.W. and H.B. Hume. 1994. Diffusion of ^{14}C in dense saturated bentonite under steady-state conditions. *Transport in Porous Media* 14, 73-84.
- Oscarson, D.W., H.B. Hume, N.G. Sawatsky and S.C.H. Cheung. 1992. Diffusion of iodide in compacted bentonite. *Soil Science Society of America Journal* 56, 1400-1406.
- Palut, J-M., Ph. Montarnal, A. Gautschi, E. Tevissnen and E. Mouche. 2003. Characterization of HTO diffusion properties by an in-situ tracer experiment in Opalinus Clay at Mont Terri. *Contaminant Hydrology* 61, 203-218.
- Rasilainen, K., K-H. Hellmuth, L. Kivedas, A. Melamed, T. Ruskeeniemi, M. Siitari-Kauppi, J. Timonen and M. Valkiainen. 1996. An interlaboratory comparison of methods for measuring rock matrix porosity. VTT Research Notes, Technical Research Centre of Finland. Espoo, Finland.
- Sawatsky, N.G. and D.W. Oscarson. 1991. Diffusion of technetium in dense bentonite. *Water, Air, and Soil Pollution* 57-58, 449-456.
- Skagius, K. and I. Neretnieks. 1982. Diffusion in crystalline rocks of some sorbing and non-sorbing species. SKB Report, 82-12, SKB/KBS, Stockholm, Sweden.
- Valkiainen, M, H. Aalto, A. Lindberg, M. Olin and M. Siitari-Kauppi. 1995. Diffusion in the matrix of rocks from Olkiluoto: The effect of anion exclusion. Nuclear Waste Commission of Finnish Power Companies Report, YJT-95-20.
- Van Loon, L.R. and J.M. Soler. 2004. Diffusion of HTO, $^{36}\text{Cl}^-$, $^{125}\text{I}^-$ and $^{22}\text{Na}^+$ in opalinus clay: Effect of confining pressure, sample orientation, sample depth and temperature. Paul Scherrer Institut, PSI Bericht Nr. 04-03.
- Van Loon, L.R., J.M. Soler and M.H. Bradbury. 2003. Diffusion of HTO, $^{36}\text{Cl}^-$ and $^{125}\text{I}^-$ in opalinus clay samples from Mont Terri. Effect of confining pressure. *Contaminant Hydrology* 61, 73-83.
- Vilks, P., J.J. Cramer, T.W. Melnyk, N.H. Miller and H.G. Miller. 1999. In-situ diffusion in granite: Phase I final report. Ontario Power Generation, Nuclear Waste Management Division Report 06819-REP-01200-0087-R00. Toronto, Ontario.
- Vilks, P., N.H. Miller and F.W. Stanchell. 2004. Phase II In-situ Diffusion Experiment. Ontario Power Generation, Nuclear Waste Management Division Report 06819-REP-01200-10128-R00. Toronto, Ontario.
- Wadden, M.M. and T.J. Katsube. 1982. Radionuclide diffusion rates in igneous crystalline rocks. *Chemical Geology* 36, 191.
- Wold, S. and T.E. Eriksen. 2000. Diffusion of organic colloids in compacted bentonite. The influence of ionic strength on molecular size and transport capacity of the colloids. SKB Technical Report, TR-00-19.

APPENDIX A: LEACH DATA TO DETERMINE PORE WATER COMPOSITION

CONTENTS

	<u>Page</u>
A.1 CALCULATION OF PORE WATER COMPOSITIONS FROM LEACHATE SOLUTIONS	59

LIST OF TABLES

	<u>Page</u>
Table A.1: Concentrations of Anions and Cations Leached from Queenston Shale	59
Table A.2: Concentrations of Anions and Cations leached from Cobourg Limestone.....	60

A.1 CALCULATION OF PORE WATER COMPOSITIONS FROM LEACHATE SOLUTIONS

Crushed rock samples were suspended in deionized water (25 mL for Queenston shale and 20 mL for Cobourg limestone) and stored in centrifuge tubes. The samples were periodically shaken to homogenize the leachate composition. The samples were allowed to leach for at least 30 days, after which they are centrifuged. The supernatant was then removed and analyzed for anions and cations. Blank solutions with deionized water and no rock sample were included to check for contamination.

The concentrations of anions and cations determined in the leachates were converted to pore water concentrations using Eq. 17, which included the sample weight, the 20 to 25 mL volume of the leaching solutions, the rock density, and the estimated sample porosity. The rock density was determined from porosity measurements, which gave average values of 2.66 for shale and 2.65 for limestone. The leached sample weights, the porosity values used, and the anion and cation concentrations determined for leach solutions are given in Table A.1 for shale and Table A.2 for limestone. The calculated pore water compositions are given in Tables 11 and 12, in the main body of the report.

$$[M]_p = \frac{[M]_L V_L \rho_{rock}}{W_S \varepsilon_c} \quad (17)$$

where:

$[M]_L$ ion concentration in leachate solution (mg/L)

$[M]_p$ ion concentration in pore water (mg/L)

V_L volume of leachate (L)

ρ_{rock} rock density (g/cm^3)

W_S weight of leached sample (kg)

ε_c rock porosity

Table A.1: Concentrations of Anions and Cations Leached from Queenston Shale

Sample Depth (m)	Porosity	Sample Weight (g)	Cl (mg/L)	Br (mg/L)	SO ₄ (mg/L)	Na (mg/L)	K (mg/L)	Ca (mg/L)	Mg (mg/L)	Sr (mg/L)
blank	-	0	<0.5	<0.5	<0.5	0.021	0.015	<0.08	<0.03	<0.004
73.584	0.060	27.7391	3590	< 3	13	1730	143	400	59	7.5
84.04	0.060	26.4946	2720	15.5	35.7	1520	121	280	39	5.8
84.064	0.060	17.8353	2100	25.1	123	1040	92	300	39	5.8
90.221	0.060	28.3232	3120	6.8	183	1590	117	380	50	8.3
101.719	0.060	23.7156	2280	24.2	240	1240	118	310	37	6.2
101.72	0.060	18.1211	1760	24.4	168	950	94	220	27	4.5
101.721	0.060	18.1442	1700	24.7	166	910	94	220	27	4.5
104.83	0.060	18.0555	1540	21	220	810	80	220	29	4.3

The volume of the leach solutions was 0.025 L.

Table A.2: Concentrations of Anions and Cations Leached from Cobourg Limestone

Sample Depth (m)	Porosity	Sample Weight g	Cl mg/L	Br mg/L	SO₄ mg/L	Na mg/L	K mg/L	Ca mg/L	Mg mg/L	Sr mg/L
blank	-	0	0.0012	0.001	<0.001	0.004	<0.0001	<0.001	<0.001	<0.0001
36.5	0.015	15.1054	657	1.22	110	210	15.8	116	41	5.3
36.5	0.015	15.6319	541	1.1	100	240	18.6	138	52	6.4
36.5	0.020	15.7683	688	1.23	139	260	18.1	138	52	7.5
36.5	0.019	15.1486	510	0.5	119	200	15.2	115	40	4.8

The volume of the leach solutions was 0.020 L.